CHEMICAL REVIEWS

Review

Cite This: *Chem. Rev.* 2018, 118, 2469–2490

pubs.acs.org/CR

Oxygen Activation and Energy Conservation by Cytochrome *c* Oxidase

Mårten Wikström,*[,†] Klaas Krab,[‡] and Vivek Sharma[†,§]

[†]Institute of Biotechnology, University of Helsinki, P.O. Box 56, Helsinki FI-00014, Finland

[‡]Department of Molecular Cell Physiology, Vrije Universiteit, P.O. Box 7161, Amsterdam1007 MC, The Netherlands

[§]Department of Physics, University of Helsinki, P.O. Box 64, Helsinki FI-00014, Finland

ABSTRACT: This review focuses on the type A cytochrome *c* oxidases (C*c*O), which are found in all mitochondria and also in several aerobic bacteria. C*c*O catalyzes the respiratory reduction of dioxygen (O_2) to water by an intriguing mechanism, the details of which are fairly well understood today as a result of research for over four decades. Perhaps even more intriguingly, the membrane-bound C*c*O couples the O_2 reduction chemistry to translocation of protons across the membrane, thus contributing to generation of the electrochemical proton gradient that is used to drive the synthesis of ATP as catalyzed by the rotary ATP synthase in the same membrane. After reviewing the structure of the core subunits of C*c*O, the active site, and the transfer paths of electrons, protons, oxygen, and water, we describe the states of the catalytic cycle and point out the few remaining uncertainties. Finally, we discuss the mechanism of proton translocation and the controversies in that area that still prevail.

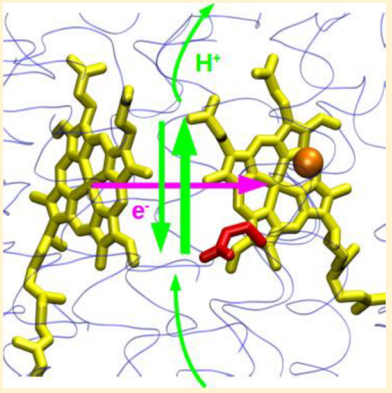

CONTENTS

1. Introduction 2469
2. General Thermodynamics 2470
3. Overall Structure of the Core Subunits 2471
   3.1. Subunit I 2471
   3.2. Subunits II and III 2472
4. Structure of the Active Site 2472
   4.1. Synthetic Models 2473
5. Paths of Electrons, Protons, Oxygen, and Water 2473
   5.1. Oxygen Channels and the Escape of Water 2474
   5.2. Electron Transfer Paths 2474
   5.3. Proton Transfer Pathways 2474
      5.3.1. D Channel 2475
      5.3.2. K Channel 2475
6. Catalytic Cycle 2476
   6.1. R and A States 2476
   6.2. P and F States 2477
   6.3. O and E States 2477
   6.4. Redox Potentials 2478
7. Proton Translocation 2479
   7.1. General Principles 2479
   7.2. Proton-Pumping Mechanism in Type A Cytochrome *c* Oxidases 2480
   7.3. Prevention of Leaks 2481
   7.4. Proposed Alternative Mechanisms 2482
      7.4.1. Role of the so-Called H-Channel 2482
      7.4.2. Linkage of the Proton Pump to the Catalytic Cycle 2482
      7.4.3. Linkage of the Proton Pump to Oxido-reduction of Heme *a* 2483
8. Conclusions in Brief 2483
Author Information 2484
   Corresponding Author 2484
   ORCID 2484
   Notes 2484
   Biographies 2484
Acknowledgments 2484
References 2484

1. INTRODUCTION

Dioxygen (O_2) is a key constituent of the Earth's atmosphere, oceans, and lakes and essential for the sustenance of all higher forms of life on the planet. The major source of O_2 is the photosynthetic water-splitting reaction of cyanobacteria and green plants. This intriguing reaction is catalyzed by a $(Mn)_4Ca$ site, the reactions of which are coupled to a photosynthetic reaction center composed of chlorophyll molecules and accompanying tyrosine and quinone species.[1−3] O_2 is thus formed as a side product of oxygenic photosynthesis. Its high oxidizing power led to a fundamental event in the evolution of life on Earth, with development of organisms capable of making use of the thermodynamic oxidation power of O_2 in harnessing a maximum amount of energy from the oxidation of the hydrocarbon foodstuffs generated via photosynthetic assimilation of CO_2. More than 90% of this O_2 consumption by living organisms is catalyzed by a superfamily of enzymes, the

Special Issue: Oxygen Reduction and Activation in Catalysis

Received: November 2, 2017
Published: January 19, 2018

DOI: 10.1021/acs.chemrev.7b00664
Chem. Rev. 2018, 118, 2469–2490

so-called heme−copper oxidases, which may be divided into three subclasses, A, B, and C.[4] They are all membrane proteins, and the oxidases of type A include the cytochrome *c* oxidases (CcO) in mitochondria and in some bacteria such as *Paracoccus dentrificans* and *Rhodobacter sphaeroides* (which are the most studied) and which are the subjects of this review. The A-type oxidases further include some quinol oxidases, notably cytochrome bo_3 of *Escherichia coli*, which has also been extensively studied.[5−7] The B- and C-type heme−copper oxidases[4] are found exclusively in bacteria and archaea and will be mentioned here only for comparative purposes. Finally, the NO reductases are also structurally related to the heme−copper oxidases and could have been their evolutionary origin.[8,9]

All heme−copper oxidases have been shown to generate a proton electrochemical gradient (protonmotive force, pmf) across the inner mitochondrial or the bacterial cell membrane and to do so by two different mechanistic means (which are intimately linked to one another). The first is due to the charge and proton separation resulting from the fact that the electrons from cytochrome *c* on the positively charged ***P*** side of the membrane are transferred to the active site of O_2 reduction within the membrane, whereas the protons required to complete the chemistry of O_2 reduction to water derive from the opposite negatively charged ***N*** side (Figure 1). In addition

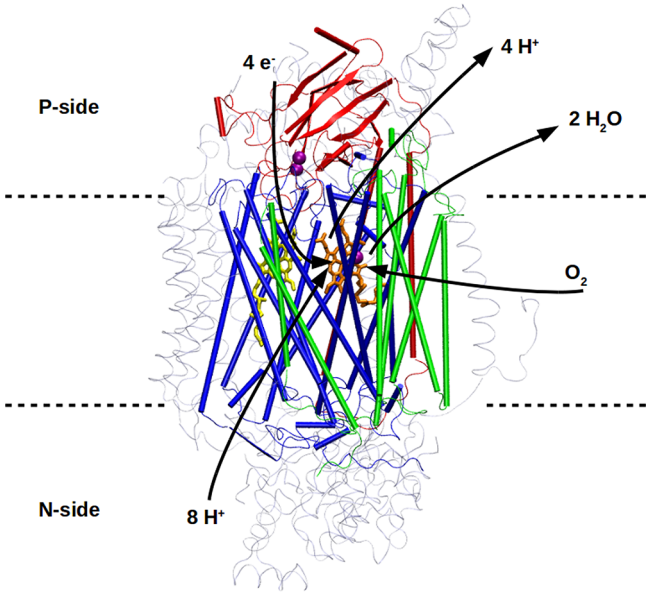

Figure 1. Thirteen-subunit A-type CcO is shown with subunits I, II, and III in blue, red, and green, respectively. Ten nuclear-coded accessory subunits are shown with transparent ribbon representation. Lipid bilayer boundaries (dotted lines) and electron, proton, and oxygen paths (arrows) are also marked. Low-spin heme (yellow), high-spin heme (orange), and copper atoms (purple) are displayed. Figure was prepared with VMD[17] software.

to this vectorial arrangement of the oxygen reduction chemistry, first suggested by Peter Mitchell,[10] all heme−copper oxidases tested to date pump up to one proton per transferred electron across the membrane from the ***N*** to the ***P*** side[11] (see Figure 1). Whereas the proton pump of the A-type cytochrome *c* oxidases, covered in this review, appears to be highly efficient with a pumping stoichiometry close to unity even at high values of the opposing protonmotive force,[11,12] the heme−copper oxidases of types B and C seem far less efficient,[13,14] and the distantly related NO-reductases do not pump protons at all.[15,16]

2. GENERAL THERMODYNAMICS

In solution, cytochrome *c* oxidase catalyzes the overall reaction

$$4\text{ferrocytochrome}\,c + 4H^+ + O_2 \rightarrow 2H_2O + 4\text{ferricytochrome}\,c \quad (1)$$

The O_2/H_2O acceptor redox couple has a midpoint redox potential at pH = 7 ($E_{m,7}$) of 815 mV. Cytochrome *c* is the donor of the four electrons, and mammalian cytochrome *c* and many bacterial *c*-type cytochromes have an $E_{m,7}$ of ca. 250 mV.[18] Hence, under standard conditions the free energy change (per electron) for reaction 1 is 565 meV (~13 kcal/mol). However, standard conditions imply an oxygen fugacity of 1 atm, which corresponds to about to 1.2 mM O_2 at 25 °C. This is a considerably higher concentration than in air-saturated water, which is 0.258 mM at 25 °C, and very much higher than typical O_2 concentrations in mammalian tissues, which vary between 0.005 and 0.025 mM.[19] The actual redox potential (E_h, relative to the hydrogen electrode) of the O_2/H_2O couple will be ~15 mV lower than the $E_{m,7}$ of 815 mV for each 10-fold decrease of $[O_2]$ below 1.2 mM, as the Nernst factor is ~60 mV/4 for a four-electron transfer reaction. A value between 785 and 800 mV thus seems reasonable for physiological conditions, and we choose 800 mV here for simplicity.

The average driving force for reaction 1 is hence ca. 800−250 = 550 meV or ~12.7 kcal/mol per electron, i.e., ~51 kcal/mol for the full four-electron reaction.

When incorporated in a membrane, cytochrome oxidase catalyzes the reaction

$$4e^-_{\boldsymbol{P}} + 4H^+_{c,\boldsymbol{N}} + 4H^+_{p,\boldsymbol{N}} + O_2 \rightarrow 4H^+_{p,\boldsymbol{P}} + 2H_2O \quad (2)$$

which distinguishes "chemical" protons (subscript c; consumed in water formation; see eq 1) from pumped protons (subscript p), which are translocated ("pumped") from the negatively charged side of the membrane (subscript ***N***) to the positively charged side (subscript ***P***). Four protons are taken up on the ***N*** side of the membrane and transported to the active site within the membrane, where they are consumed in forming water from reduced dioxygen. This is made possible by transfer of four electrons to the active site from cytochrome *c* on the ***P*** side of the membrane. In addition, remarkably, four protons are pumped across the membrane for each O_2 molecule reduced. Thus, a total of 8 electrical charges are translocated across the membrane per O_2 molecule reduced (see Figure 1).

The overall protonmotive activity of cytochrome oxidase is equivalent of pumping two protons across the membrane per transferred electron (eq 2) even though only one proton per electron is released on the ***P*** side. The uptake of electrons and protons for the catalytic chemistry of cytochrome oxidase from opposite sides of the membrane is thermodynamically equivalent to pumping of one proton across the membrane per electron, and the proton pump function contributes with a second proton. Protons released on the ***P*** side do not usually contribute significantly to the ΔpH term of the pmf since the aqueous phase on the ***P*** side is usually well buffered and/or very large in volume compared to the ***N*** side. The ΔpH term of the pmf is hence almost entirely due to the consumption of protons on the ***N*** side of the membrane.

DOI: 10.1021/acs.chemrev.7b00664
Chem. Rev. 2018, 118, 2469−2490

In mitochondria, the proton electrochemical gradient (pmf) is some 200−220 mV in the so-called State 4, where lack of ADP limits the rate of respiration and the pmf is maximal. The pmf decreases to ca. 150 mV during active ATP synthesis when there is an excess of ADP and inorganic phosphate (State 3).[20] At the thermodynamic stoichiometry of 2 H^+/e^- (see above) cytochrome *c* oxidase would thus require a minimum redox driving force of 400−440 meV to generate the maximum pmf. The mean driving force of ca. 550 meV from the oxidoreduction chemistry (see above) is hence sufficient and would point at an energy transduction efficiency of ca. 70−80% at maximum load. Careful measurements of the ATP/O (ATP/$2e^-$) ratio in mitochondria respiring only via cytochrome *c* oxidase, for example, by Hinkle[20] and Chamalaun and Tager,[21] yielded values of 0.98 and 0.94, respectively. From these values and the H^+/ATP ratio of 3.67 in animal mitochondria (2.67 H^+/ATP based on the structure of the c ring of the ATP synthase,[22] plus 1 H^+/ATP due to the coupling of ADP/ATP exchange and transport of inorganic phosphate to translocation of 1 H^+),[23] one may deduce the effective $H^+/2e^-$ ratio of proton translocation by mitochondrial cytochrome *c* oxidase on the basis of

$$H^+/2e^- = H^+/ATP \times ATP/2e^- \quad (3)$$

which yields 3.45−3.60, indicating a stoichiometric efficiency of 86−90% under the conditions of ATP synthesis, i.e., at a less than maximum load from the protonmotive force (ca. 150 mV).

3. OVERALL STRUCTURE OF THE CORE SUBUNITS

Mitochondrial C*c*O contains three core subunits (named subunits I, II, and III) that are encoded in mitochondrial DNA (mtDNA). The homologues of these three subunits are also found in all bacterial heme−copper oxidases (HCO) of type A, which apart from C*c*O enzymes also comprise quinol oxidases such as cytochrome bo_3 from *E. coli*.[4,8,9] In addition, mitochondrial C*c*Os contain up to 10 nuclear encoded "accessory" subunits (Figure 1), whose presumably regulatory functions are still poorly understood[24,25] and which are not reviewed here. HCOs of type B and C, found in bacteria and archaea (though no archaeal C-type oxidases are known), lack subunit III, which is thus unique for the type A HCOs. Variations among B and C enzymes also exist with regard to subunit II, which is in many cases replaced by heme *c*-containing proteins.[4] However, a homologue of subunit I is conserved in all HCOs and even in the distantly related NO reductases.[4,9] This review focuses on the C*c*O enzymes of type A, which includes mitochondrial cytochrome *c* oxidase; B- and C-type HCOs (and the NORs) will be mentioned only for comparative purposes. All amino acid numbering corresponds to type A C*c*O from *Bos taurus* mitochondria, unless mentioned otherwise.

3.1. Subunit I

The cylindrically shaped catalytic subunit I of C*c*O has a highly conserved characteristic fold found in all HCOs. The 12 transmembrane helices are slightly tilted with respect to the membrane normal and are arranged in three clusters with a quasi-3-fold symmetry[26] (Figure 2A). Each of the three helical clusters house a hydrophilic pore, shown by a cyan-colored circle in Figure 2A, which contains polar amino acid residues and water molecules. Two of the pores are known to transport protons required for oxygen reduction and proton pumping at least in the bacterial A-type oxidases, whereas the function of

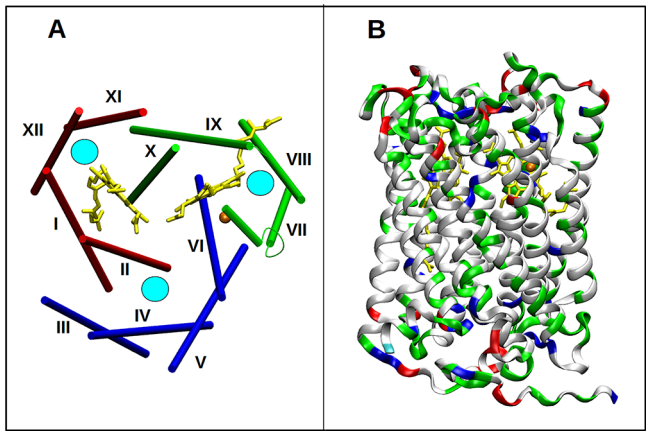

Figure 2. (A) View of the catalytic subunit I from the ***P*** side of the membrane. Three helix clusters III−VI, VII−X, and XI, XII, I and II are shown in blue, green, and red, respectively. Two clusters (green and red) hold the redox-active centers. Three pore regions (filled circles) are found in each of the three clusters. (B) Side view of the cylindrically shaped catalytic subunit. TM helices are shown as ribbons, colored according to residue polarity (polar, green; acidic, red; basic, blue; hydrophobic, white). Hemes (yellow) and Cu_B (orange), buried in the catalytic subunit, are also displayed.

the third pore domain is controversial. It includes the so-called H channel that has been claimed to be the exclusive proton pump pathway in the mammalian mitochondrial oxidase (see section 7.4.1).

Two of the helical clusters (red and green, Figure 2A) hold the buried redox centers, the low-spin heme, and the high-spin heme plus Cu_B, which are all ligated by histidine residues from subunit I (Figure 3A and 3B). These six histidine ligands are

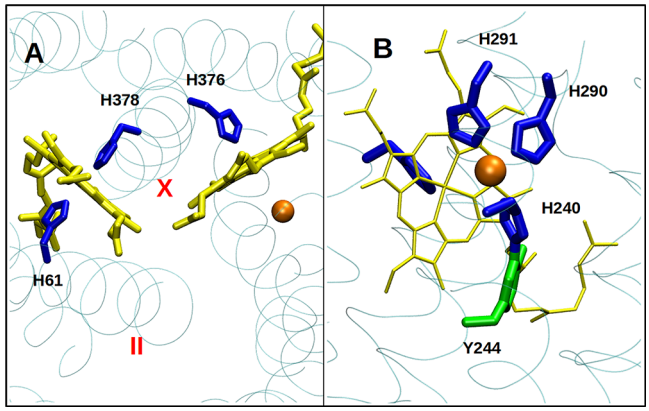

Figure 3. (A) Top view (from the ***P*** side of the membrane) showing histidine ligands of heme cofactors. Two TM helices in subunit I (II and X) that carry conserved histidine residues are marked in red. (B) Side view showing the histidine ligands of the Cu_B center. Two tandem histidines (H290 and H291) originate from helix VII, whereas the His240-Tyr244 cross-link is from helix VI. As before, hemes and Cu_B are shown in yellow and orange.

fully conserved in the HCO superfamily, and their spread along the entire sequence of subunit I has played an important role in earlier sequence alignment and homology modeling studies.[4,27]

The majority of subunit I secondary structure comprises transmembrane (TM) helices that face the lipid bilayer or TM domains of noncatalytic accessory subunits. These interactions are predominantly nonpolar in nature, whereas the loop regions

DOI: 10.1021/acs.chemrev.7b00664
Chem. Rev. 2018, 118, 2469−2490

that extend into the positively charged ***P*** and negatively charged ***N*** phases on both sides of the membrane comprise charged or polar amino acid residues (Figure 2B).

3.2. Subunits II and III

Subunit II consists of three major structural components, two TM helices and one β-sheet cluster consisting of 10 sheets (Figure 4A). The two TM helices make extensive contacts to

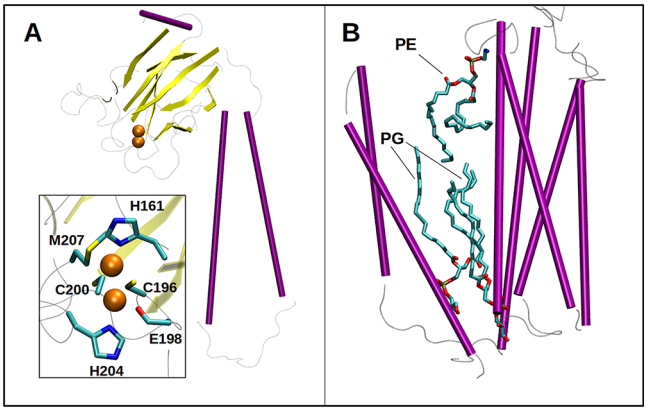

Figure 4. (A) Structure of subunit II. (Inset) Cu_A center and its ligand sphere. (B) Structure of subunit III. α-Helices and β-sheets are shown in purple and yellow, respectively. Amino acid residues are marked with their one letter codes and numbers. Phosphatidylglycerol (PG) and phosphatidylethanolamine (PE) lipid molecules bound to subunit III are displayed in licorice representation.

the TM helices VIII and IX of subunit I, whereas the β-sheet cluster on the ***P*** side of the membrane holds the dimetallic Cu_A center, which is the first electron acceptor from cytochrome *c* (Figure 4A, inset). The role of subunit II in electron transfer to the catalytic subunit is well known. Additionally, due to the presence of a conserved acidic residue (Glu62 in *B. taurus*) in the second TM helix of subunit II, its role in proton uptake has also been implicated[7,28,29] (see section 5.3). The subunit I/II interface is partly bridged by a magnesium ion, which is ligated by conserved residues from both subunits but which is absent from the type A quinol oxidases[5] as well as from the HCOs of type B and C.

Subunit III is highly conserved but found exclusively in the A-type oxidases. It consists of 7 TM helices divided into two clusters of 2 and 5 helices each, forming a V-shaped structure (Figure 4B), except for the case of the quinol oxidase bo_3. In this latter case, two of the TM helices that are "normally" parts of subunit III are linked with subunit I instead but attaining positions in the 3D structure very similar to the case of the cytochrome *c* oxidases of family A.[5]

Subunit III makes extensive hydrophobic contacts with subunit I. It does not contain any redox-active cofactor and plays no direct role in redox-coupled proton pumping.[30] However, it provides stabilization to the two-subunit enzyme by enhancing the number of turnovers by preventing suicide inactivation.[31−33] As shown by the extensive work of Hosler et al.,[31−33] the suicide inactivation of C*c*O is enhanced under conditions where the local proton activity near the BNC is low. Under such conditions of limited H^+ access Cu_B may acquire two hydoxide ligands and leave the structure as copper hydroxide. The suicide inhibition has indeed been shown to be caused by depletion of Cu_B from the enzyme.[33] One role of subunit III is presumably to prevent this effect by enabling fast H^+ uptake to the BNC via the D pathway, even at relatively high values of pH of the ***N*** phase (see below).

The architecture of subunit III is also unique in the sense that it contains three tightly bound lipid molecules, stabilized by polar and nonpolar interactions. The lipid-binding site region has been proposed to play an important role in O_2 channeling (see section 5.1),[34] whereas the charged head groups of the tightly bound lipids may enhance the rate of proton transfer by perturbing the pK_a of Asp91, the proton uptake site of the proton-conducting D channel.[35] Like subunit III, the D channel is also unique for the A-type HCOs.

4. STRUCTURE OF THE ACTIVE SITE

The catalytic subunit I of C*c*O houses the active site for oxygen reduction, the so-called binuclear center (BNC). The key components of the BNC are two magnetically coupled redox-active metal centers, a high-spin heme (a_3) and a copper ion (Cu_B). The high-spin heme is bound to the protein matrix by means of covalent and noncovalent interactions. On its proximal side, the heme iron is ligated by a highly conserved histidine residue (H376) from helix X (Figure 3A). On the distal side, between the iron and the Cu_B, small diatomic ligands such as CO, CN^-, and the physiological substrate O_2 bind axially to the Fe (see below). The two propionate groups of the high-spin heme interact electrostatically with titratable amino acid residues from subunit I (Figure 5), whereas the heme macrocycle is buried between nonpolar residues. The strong electrostatic interactions between the negatively charged propionate groups and the conserved amino acids are known to be important for the proton-pumping function of the

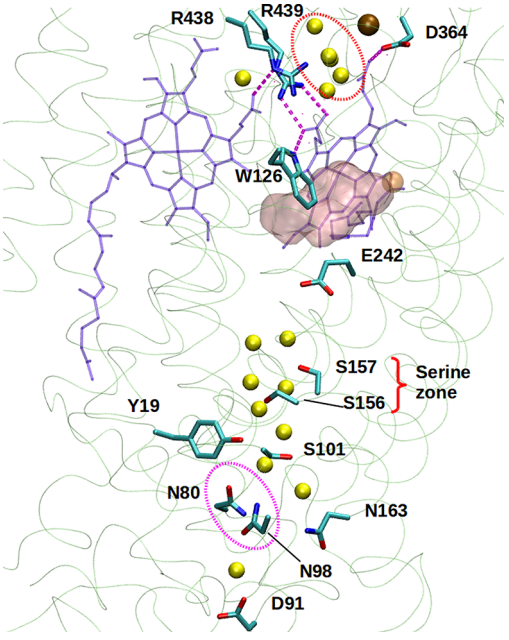

Figure 5. Proton-pumping elements in HCO of type A. The D channel of proton transfer is displayed, which comprises the proton-uptake site (D91), the asparagine gate (circled with purple dotted line), the serine zone, and a highly conserved acidic residue, Glu-242. Heme propionate region is highly polar and consists of a water cluster (circled with red dotted line), two arginines, and one acidic residue, Asp-364. Water molecules (yellow), hemes (blue, left, heme *a*; right, heme a_3), Cu_B (orange), Mg ion (brown), and subunit I (green transparent ribbons) are also shown. Nonpolar cavity where water produced at the active site may be released is shown as a pink "cloud".

DOI: 10.1021/acs.chemrev.7b00664
Chem. Rev. 2018, 118, 2469−2490

Table 1. Metal−Metal and Edge−Edge Distances (in Angstroms) between the Redox Centers of Enzymes from Different HCO Subfamilies

subfamily	PDB id	organism[a]	distance[b]	distance[c]	distance[d]
A	5B1A	Bt	19.41 (11.82)	13.20 (6.77)	4.83
A	2GSM	Rs	19.36 (11.82)	13.22 (6.95)	4.89
A	3HB3	Pd	19.45 (12.06)	13.27 (6.73)	4.62
A (quinol oxidase)	1FFT	Ec		13.69 (7.79)	5.30
A (caa_3 type)	2YEV	Tt	19.47 (11.99)	13.58 (7.11)	4.85
B	3S8F	Tt	19.07 (11.97)	13.70 (7.36)	4.87
C	3MK7	Ps	19.75 (11.65)	13.05 (6.00)	4.58
*c*NOR	3WFD	Pa	20.45 (13.34)	13.88 (6.49)	4.43
*q*NOR	3AYF	Gs		13.73 (6.30)	4.58

[a]Bt, *Bos taurus*; Rs, *Rhodobacter sphaeroides*; Pd, *Paracoccus denitrificans*; Ec, *Escherichia coli*; Tt, *Thermus thermophilus*; Ps, *Pseudomonas stutzeri*; Pa, *Pseudomonas aeruginosa*; Gs, *Geobacillus stearothermophilus*. [b]Metal-to-metal (edge-to-edge) distance between Cu_A and heme *a* in A- and B-type oxidases, and same distance between heme *c* and heme *b* in C-type oxidases and *c*NORs. [c]Fe−Fe distance between low-spin and high-spin heme (edge−edge distance in parentheses), [d]Distance between the two metals of the BNC

enzyme.[36−40] In between the two propionates is a cluster of crystallographically visible water molecules (Figure 5).

The high-spin heme sits next to the redox-active Cu_B center, with the two metals (Fe and Cu) only ∼5 Å apart (see Table 1). The Cu_B center has a unique structural arrangement in which the copper ion is ligated by two vicinal histidines (H290 and H291 from helix VII of subunit I) and by another histidine (H240) which is covalently linked to a functionally critical tyrosine (Y244). It is important to realize that this tyrosine is part of the unique his-tyr ligand of Cu_B (Figure 3B). Both this histidine and the tyrosine are part of a highly conserved sequence motif in helix VI of subunit I of the A-type oxidases, -G**H**PEV**Y**-. High-resolution crystal structures of bovine oxidase show that the three histidine nitrogens ligating the copper atom are nearly planar forming a T-shaped structure,[26,41,42] an arrangement preferred by reduced, cuprous copper (Cu[I]). In higher oxidation states, the copper center apparently loses planarity, with a water or a hydroxyl ion positioned as the fourth ligand.[43,44] Recent biosynthetic and theoretical work has provided explanations for why the copper is preferred over iron in O_2 activation and reduction.[45] The crystal structure data of the fully oxidized enzyme shows electron density between the two metals (Fe and Cu), suggested to be a bound peroxide.[46,47] However, an unambiguous assignment cannot be made, and the exact identity of the ligand structure between Fe and Cu in the fully oxidized state of the enzyme remains under debate.[48]

Besides the ligand bridge, heme a_3 and Cu_B also interact by means of an H bond between the hydroxyl of the hydroxyethylfarnesyl chain of heme a_3 and the side chain of Y244. The functional role of this interaction is not known but may be important in modulating the pK_a of the tyrosine. The histidine-tyrosine cross-link is a highly conserved motif in the A-, B-, and C-type oxidases, and its role in catalysis is also established (see section 6). Interestingly, in the C-type oxidases, the cross-linked tyrosine originates from a different helix (helix VII instead of helix VI) and adopts a configuration slightly different from what is observed in the A- and B-type oxidases[27,49] (see also refs 50−52). This coincides with the absence of a hydroxyl group on the high-spin heme, which is protoheme or heme B in the C-type oxidases, and may be important in tuning the redox and acid/base properties of the cross-linked tyrosine in C-type oxidases.[53]

The basic BNC structure just described is shared by the distantly related nitric oxide reductases (NORs), consisting of the cytochrome *c*- and quinol-dependent NORs. However, there are key differences. One is the replacement of the Cu_B ion with an Fe ion, and the second is the presence of a glutamate ligand to the Fe_B center in *c*NORs, which is replaced by water molecules in *q*NORs.[54−56] Moreover, there is no redox-active tyrosine in the vicinity of the active site in the NORs. Structural and functional studies on NORs remain an active area of research.[57,58]

4.1. Synthetic Models

Synthetic heme−copper oxidase adducts have played an important role in shedding light on the oxygen reduction reaction.[59,60] Early on structural and kinetic analysis on heme−copper oxidase model compounds led to the identification of two stable species: μ-oxo (Fe[III]−O−Cu[II]) and μ-hydroxo (Fe[III]−OH−Cu[II]).[61,62] Even though such species have not yet been observed experimentally in the molecular mechanism of C*c*O, the latter has nevertheless been predicted to occur based on DFT calculations[63−65] in the fully oxidized activated form of the enzyme (O_H, see section 6.3). It is also interesting to note that the presence of a true peroxy intermediate (O_2^{-2}) has never been observed experimentally in the catalytic reaction of C*c*O[66] (see also ref 67) even though quantum chemical calculations on the conversion of state A to state P in the catalytic cycle (section 6) supports its presence.[53,68] In contrast, a peroxy species is readily observed in the oxygen reduction reaction of heme−copper oxidase mimics and exists in two structurally distinct forms, side on and end on.[69]

Recent work in synthetic chemistry has shown that artificial chemical constructs that mimic the active site of cytochrome *c* oxidase are able to catalyze the reaction with a high turnover number.[70] Furthermore, such approaches have highlighted the importance of H bonding in the O−O bond cleavage reaction, such that a phenolic group may assist in further reducing the bound peroxide by supplying an electron and a proton to it.[71,72] Earlier, density functional theory (DFT) calculations performed on A- and C-type oxidases model systems have indeed shown the functional importance of such an H-bonding arrangement between the bound O_2 molecule and the cross-linked Tyr, also through a mediating water molecule.[53,73] It is likely that such an H-bonding arrangement enhances the rate of proton-coupled electron transfer necessary for O−O bond cleavage.

5. PATHS OF ELECTRONS, PROTONS, OXYGEN, AND WATER

Reduction of molecular oxygen to water at the active site requires three reactants, molecular oxygen (O_2), electrons (e^-),

DOI: 10.1021/acs.chemrev.7b00664
Chem. Rev. 2018, 118, 2469−2490

and protons (H^+), and yields a single product water if one ignores the net translocation of protons. All of the above differ greatly in their mass, charge, and chemical properties. Therefore, it is not surprising that the paths taken to reach and leave the active site are also quite different.

5.1. Oxygen Channels and the Escape of Water

Due to its apolar nature the O_2 molecule is much more soluble in lipid membranes than in the surrounding aqueous phases and is found to localize at the center of the lipid bilayer.[74−76] In the middle of the membrane two sets of TM helices of subunit III of the A-type oxidases form a V-shaped structure surrounding a hydrophobic channel in subunit I, which leads from the membrane interior to the active site buried in the interior of the enzyme. This path has been identified as an O_2 channel, based on crystal structure data[77] and kinetic experiments.[34] Xenon-labeling experiments with cytochrome aa_3 from *Rh. sphaeroides*[78] and the B-type cytochrome ba_3 from *T. thermophilus*[79,80] have confirmed and extended this conclusion.

Two water molecules are produced at the BNC in each catalytic cycle. By labeling O_2 with ^{17}O Ferguson-Miller et al.[81] showed by paramagnetic resonance spectroscopy that the labeled product water reached the Mg site (see Figure 5), which was substituted by a manganese ion in the experiment, within milliseconds of the reaction with O_2. This finding was supported by computational work[37] that suggested how water produced at the BNC would reach the Mg domain above the hemes via dissociation of the delta-propionate (heme a_3)-arginine ion pair (see purple dotted lines between R438 and heme-propionate in Figure 5). Facile water access between the BNC and the Mg domain may be expected to lead to uncoupling pathways of protons, so such a pathway of water transport must be carefully controlled (gated). The computational studies[37] indeed indicated that dissociation of the propionate-arginine ion pair was strongly dependent on the redox state. In addition, redox-dependent water dynamics in a tight nonpolar confinement (Figure 5) and hydration/dehydration transitions may also be expected to prevent such an uncoupling (see also ref 82).

5.2. Electron Transfer Paths

Electrons as elementary particles are often described by the wave−particle duality. In the context of electron transfer in proteins, both the wave (dynamic electron tunneling) and the particle (equilibrium redox potential) nature of the electrons are at play. Long-range electron transfer in proteins is accomplished through buried metal centers, which are bound to the protein matrix. A wide variety of metal centers are found in redox-active proteins, such as hemes, coppers, iron sulfur clusters, manganese clusters, etc. A survey of a large number of crystal structures of redox-active proteins has revealed that electron transfer at biologically relevant rates takes place through redox centers that are placed not more than ca. 14 Å apart when measured edge-to-edge.[83] The process of electron transfer in proteins through fixed redox centers is relatively well understood.[83,84] It seems that the nature of the intervening proteinaceous medium in electron transfer between the electron donor and the electron acceptor groups is of relatively little importance in practice.[85] Although electron transfer rates do depend on the medium structure[86] and electron transfer calculations may reveal preferred pathways, for example, in C*c*O,[87] it seems that the number of relevant pathways between the donor and the acceptor becomes very high in proteins, especially at longer distances. Under such circumstances it is the distance not the medium composition that is the main determinant of the rate of electron transfer.

Electron transfer in C*c*O is initiated with the formation of a cytochrome *c*−C*c*O (donor−acceptor) complex. Reduced cytochrome *c* binds on the surface of subunit II on the ***P*** side of the membrane and donates an electron to the Cu_A center of the enzyme. The detailed nature of this step was recently elucidated from the crystal structure of a complex between cytochrome *c* and C*c*O.[88] The interface between the two proteins is found to be stabilized by weak electrostatic interactions, enabling rapid association and dissociation of the donor−acceptor complex, in agreement with earlier kinetic experiments and modeling approaches.[89−91] The crystal structure of the complex identified a new class of protein−protein interaction termed "soft and specific", which had not been previously predicted.[92]

The intraprotein electron transfer processes in C*c*O are relatively well understood. The primary electron acceptor is a cupredoxin-type center, Cu_A, which consists of two closely spaced (~2.5 Å) copper atoms, each ligated by a cysteine and a histidine residue from subunit II. Cu_A undergoes a one-electron redox transition that can formally be written as $Cu^{II}/Cu^{II} + e^- \leftrightarrow Cu^{I}/Cu^{II}$, while the Cu^{I}/Cu^{I} structure is too high in energy to be occupied. The edge-to-edge distances from the Cu_A center to heme *a*, heme a_3, and Cu_B are ca. 12, 16, and 20 Å, respectively. Thus, the bis-imidazole-ligated low-spin heme *a* located approximately 1/3 into the membrane will be the acceptor of the electron from Cu_A in a pure electron tunneling event with a time constant (τ = inverse rate constant, $1/k$) of ca. 10−50 μs depending on the source of enzyme.[93] The rate is insensitive to variations in pH and to heavy water substitution and fits very well with the rate of 8.7×10^4 s^{-1} ($\tau \approx 11$ μs) predicted by the Moser−Dutton ruler.[85] In equilibrium titrations, however, the redox potential of heme *a* has been found to be weakly linked to nonstoichiometric proton uptake especially when heme a_3 and Cu_B are oxidized (ca. 0.4 H^+).[94]

Pure electron transfer, not coupled to any proton transfer or conformational change, from the electron-queueing heme *a* to the BNC occurs by nanosecond electron tunneling.[95,96] This is due to the fact that the hemes *a* and a_3 are very closely spaced with only a 7 Å (edge-to-edge) distance between them. During enzymatic turnover, it is this electron transfer step that has been found to drive the internal proton transfer step that initiates the proton-pumping function (see section 7.2).[97]

5.3. Proton Transfer Pathways

The proton is 1837 times heavier than the electron and cannot tunnel across distances longer than 1−2 Å on biologically relevant time scales (see ref 93). However, long-range proton transfer (tens of Angstroms) is typical of biological systems such as respiratory and photosynthetic complexes.[98] Therefore, some sort of "medium" is necessary to accomplish proton transfer across longer distances. It is observed in crystal structures of several enzymes involved in redox-coupled proton transfer that there are cavities of varying sizes and volume formed by surrounding charged or polar amino acids that can hold bound water molecules.[99,100] Combined with site-directed mutagenesis studies, some of these hydrated cavities have been identified to function as proton transfer pathways in A-type oxidases,[6,101−105] but they may also have other roles such as "dielectric wells".[106,107] Proton transfer in such pathways occurs

DOI: 10.1021/acs.chemrev.7b00664
Chem. Rev. 2018, 118, 2469−2490

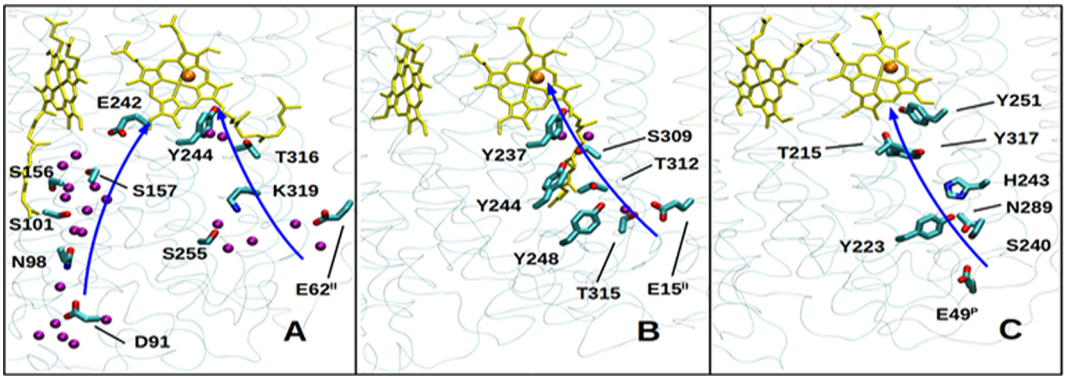

Figure 6. Proton transfer pathways in type A (A), B (B), and C (C) HCOs.

by means of the classical Grotthuss mechanism described in detail elsewhere.[108]

In HCOs, proton channels are responsible for the transfer of protons from the ***N*** side of the membrane to the site of O_2 reduction and for pumping from the ***N*** to the ***P*** side of the membrane (Figure 1). The proton pump mechanism requires a proton-loading site (PLS, also called pump site or proton trap). In its simplest form the PLS accepts a proton from the ***N*** side under conditions where it is isolated protonically from the ***P*** side and donates the proton to the ***P*** side under conditions where it is isolated from the ***N*** side. Thus two separate proton channels are required for the proton-pumping process: one from the ***N*** side of the membrane to the PLS and another from the latter to the ***P*** side. The former is relatively well defined (section 5.3.1), whereas the latter is still poorly understood.

5.3.1. D Channel. One of the best characterized proton transfer pathways in the A-type oxidases is the D channel, which is named after the highly conserved residue D91 at the ***N*** side surface of subunit I (Figures 5 and 6A). Already before the availability of the crystal structures, biochemical experiments revealed the importance of this aspartate in proton transfer linked to the proton-pumping activity.[6] The D channel begins at the ***N*** side of the membrane with the solvent-exposed D91 forming the proton uptake site. Lined with a number of water molecules and polar amino acid residues, the channel continues inside the protein up to about halfway into the membrane (Figure 6A). Above D91, two conserved asparagine residues appear to form a gate.[109,110] Site-directed mutagenesis of several conserved amino acid residues of the D channel has led to interesting phenotypes.[111,112] For example, mutation of N98 (N139 in enzyme from *Rh. sphaeroides*) to an aspartate leads to decoupling of the oxygen reduction reaction from proton pumping so that the latter is completely abolished. The molecular reasons for this unusual effect are being actively discussed.[110,113]

The D channel ends at a highly conserved acidic residue, E242, from where it is unclear from the crystal structures how protons are transferred to the active site (substrate protons) and for pumping to the ***P*** side. Between E242 and the heme groups "above" the glutamic acid there is an apolar cavity that appears empty in all crystal structures to date (Figure 5). Computational approaches provided key insights into how protons could be transferred further, viz. by side chain conformational transitions of E242,[114,115] and dynamic water molecules in the cavity above it.[82,116,117] Several research groups have proposed a functional role of water molecules transiently present in this cavity.[118−122] Overall, the kinetics of proton transfer through the D channel and its role in supply of at least two substrate and all four pumped protons is well established from functional site-directed mutagenesis experiments on A-type cytochrome *c* and quinol oxidases from bacteria[123] and from yeast mitochondria.[124] By contrast, Yoshikawa and colleagues claim that the translocation of the pumped protons in mammalian mitochondrial C*c*O, which are also of type A, does not occur via the D pathway but via another pathway—the H channel (see section 7.4.1).

Crystal structures,[5,78,125−128] site-directed mutagenesis,[129,130] and molecular dynamics simulation studies[131] reveal that a proton channel analogous to the D channel is unique for the A-type heme−copper oxidases and is entirely lacking from the B- and C-type oxidases. It seems that this "deficiency"—and the lack of subunit III—may be related to the relatively poor proton-pumping efficiency of the latter oxidases[14] compared to the high efficiency of the A-type enzymes. We argued[13,132] that this suggests that the B- and C-type enzymes are more ancient in evolution compared to the enzymes of type A, but this view is not fully accepted.[133]

5.3.2. K Channel. The K channel in the A-type C*c*Os is based on a highly conserved lysine residue (K319), which when mutated to a nonpolar residue completely abolishes catalytic turnover.[106] Similar to the D channel, an acidic residue (from subunit II) forms the putative proton uptake site at the ***N*** side of the membrane[28,134] (see Figure 6). The K channel terminates close to the BNC near the cross-linked tyrosine, which forms an H bond with the hydroxyl of the hydroxyethyl farnesyl side chain of the high-spin heme a_3. It has been proposed that the K channel supplies one or two substrate protons in the reductive phase of the catalytic cycle (see section 6). In comparison to the highly hydrated D channel, the K channel comprises fewer predicted water molecules and is also scarce in polar amino acid residues[26,126] (Figure 6A). In all resolved crystal structures of A-type oxidases, lysine (K319) adopts a conformation in which its side chain is ca. 18 Å from the BNC. However, experiments and computer simulation studies have led to the proposal that the lysine side chain may undergo an "up-flip" that brings it closer to the BNC by ca. 5 Å and which may be important for the proton-pumping function of the enzyme[126,135−137] (section 7.2).

A wide variety of ligands are known to bind to the region next to the K channel, as observed crystallographically and also characterized biochemically.[43] This has led to the suggestion that the proton transfer through the K channel is regulated.[43] Despite a vast amount of literature on K channel structure and function, its precise role remains unclear. In other words, it is

DOI: 10.1021/acs.chemrev.7b00664
Chem. Rev. 2018, 118, 2469−2490

not known why this channel is needed in addition to the D channel and why it supplies only some of the substrate protons (see the computational work by Blomberg and Siegbahn[138] and Sharma and Wikström[136]). It is also unclear how it operates together with the D channel. Nevertheless, the pore of the channel, formed by the polar residues from helices VIII and IX of subunit I (Figure 2), is conserved in all three subfamilies (type A, B, and C; see also panels A, B, and C in Figure 6), suggesting that this proton transfer route may have existed in the earliest forms of HCOs.[27]

In the B- and C-type oxidases, which lack the D channel altogether, the K channel analogue is responsible for the transfer of both the substrate and the pumped protons[129,130] (Figure 6B and 6C). Site-directed mutagenesis as well as molecular dynamics simulation studies on C-type oxidases have provided significant insights into the putative proton transfer paths for substrate and pumped proton transfer.[131,139] The situation is less clear in the B-type oxidases, which are also bona fide proton pumps. While the route of proton uptake is biochemically tested[129] and also analyzed through molecular simulations,[140] the way the protons are gated toward the ***P*** side of the membrane remains unclear.

6. CATALYTIC CYCLE

6.1. R and A States

The states of the catalytic cycle as discussed here (Figure 7) as well as elsewhere refer primarily to the structure of the

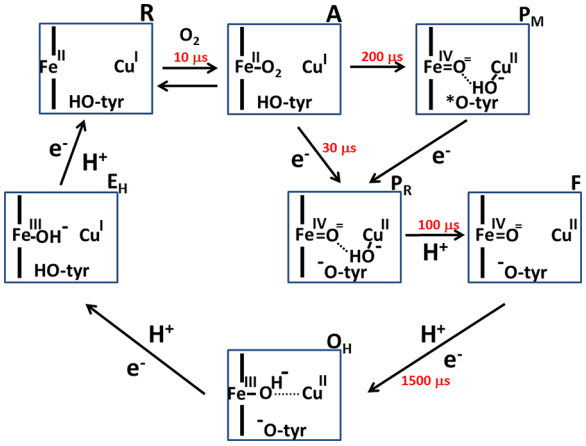

Figure 7. Catalytic cycle. Square encompasses the binuclear site with the heme a_3, Cu_B, and the covalently linked tyrosine (HO-tyr). Distal histidine ligand of heme a_3 and the three histidine ligands of Cu_B are not shown for simplicity. Uptake of protons to complete the chemistry of water formation is shown, but proton pumping is not shown. One proton is pumped across the membrane in each of the one-electron reactions, but for the A → F reaction the situation is more complicated: formation of state P_R is linked to loading the PLS from the ***N*** side of the membrane; its release to the ***P*** side is driven by uptake of the chemical proton in formation of state F (see text). Structures of intermediates R, A, P_M, P_R, and F are well established (see text), whereas those of states O_H and E_H are still more hypothetical.

binuclear iron−copper center, including the adjacent tyrosine residue that is covalently linked to one of the histidine ligands of Cu_B. In the R (reduced) state the ferrous heme a_3 is five-coordinated high spin and the Cu_B is cuprous (Cu_B[I]). In this state the heme readily binds ligands, such as O_2, CO, and NO, which results in a high- to low-spin transition that is revealed by MCD, magnetic susceptibility, and optical experiments.[141,142] Interestingly, the binding of ligands such as O_2 to ferrous heme a_3 seems to occur only under conditions where the nearby Cu_B is also reduced.[143] A possible reason for this is that the fourth OH^- ligand of Cu_B[II] prevents access to the iron of heme a_3 and is only removed by protonation to water that readily dissociates upon reduction of the copper.

Binding of the physiological ligand O_2 to the originally five-coordinated iron of heme a_3 results in the so-called A state, originally named Compound A by Britton Chance et al.,[144] who first demonstrated this state experimentally in low-temperature optical experiments.

The resonance Raman (RR) band of state A at 571 cm^{-1} (Table 2; see Ferguson-Miller and Babcock[142]) is indicative of

Table 2. Spectroscopic Data on Key Intermediates of the Catalytic Cycle

intermediate	resonance Raman Fe−O vibration (cm^{-1})	light absorption maxima (nm)[a]
A (Fe[II]−O_2)	571	590, 430
P (Fe[IV]═O)	804	607, 442
F (Fe[IV]═O)	785	580, 442
O_H (Fe[III]−OH)	450	NA, NA

[a]In a difference spectrum vs the O state. References to this data are found in the main text.

binding O_2 "end on" to the iron by comparison to the spectra and crystal structures of HbO_2, and this binding geometry was proven by the elegant RR work of Kitagawa and Ogura[145] using $^{16}O-^{18}O$-labeled O_2, by which a "side on" geometry could be excluded. On the basis of quantum-chemical calculations the A intermediate is an $S = 0$ open-shell singlet biradical state (Figure 8). The O−O bond length is intermediate between free

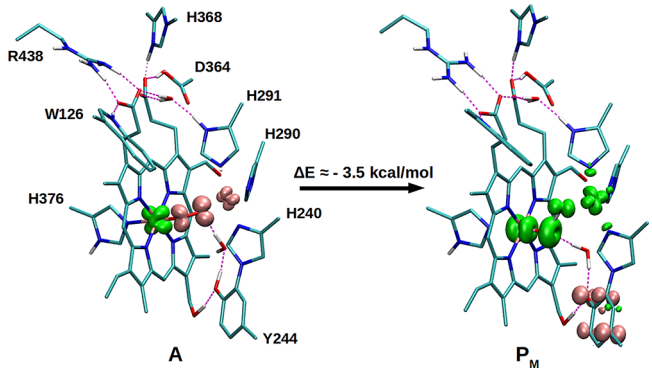

Figure 8. Oxygen-splitting A → P_M transition. Density functional theory-based geometry optimizations (def2-SVP/TZVP/BP86/disp3/MARIJ)[148−154] and energy calculations (def2-TZVP/B3LYP/disp3/eps4)[148,149,151,152,155−157] were performed with Turbomole[158] software on large model systems of the BNC. Spin density (α, green; β, pink) are plotted at an isosurface value of 0.01 e/Å^3.

dioxygen and peroxide and may best be regarded as a superoxide coordinated to a ferric iron, even though the state is often abbreviated as ferrous−oxy, Fe[II]−O_2. The spin distribution shows that the iron is low-spin ferric antiferromagnetically coupled to the unpaired electron located on the two oxygens of superoxide.[146,147]

At room temperature and at 1 mM O_2, state A is formed with a time constant of ca. 10 μs.[159] Prior to this O_2 diffuses to the

DOI: 10.1021/acs.chemrev.7b00664
Chem. Rev. 2018, 118, 2469−2490

active site from the lipid membrane, where it is dissolved at a concentration at least ca. 5-fold higher than in the surrounding aqueous phases.[74−76] The diffusion occurs via channels in the structure of subunit I that have been clearly identified from the X-ray diffraction data as well as from mutagenesis experiments (see section 5.1). The second-order rate constant for O_2 binding is 1.38×10^8 M^{-1} s^{-1}, and the dissociation constant (K_D) is as high as 0.28 mM, which means that the off rate is ca. 40 000 s^{-1}. At an O_2 concentration of 100 μM ([O_2] in tissues is usually in the range 5−25 μM (see ref 19)) the free energy change of dioxygen binding is ca. +0.6 kcal/mol. These apparently unfavorable numbers are traded off kinetically by fast "trapping" of the O_2 once bound by electron transfer,[160] which renders the apparent Michaelis constant to be 3 orders of magnitude lower than K_D. Blomberg et al. reported a calculated free energy change of −1 kcal/mol for the R → A reaction step, but this was based on a 1 mM activity of O_2.[161]

6.2. P and F States

There are two kinds of P states which were named such because the structure of the BNC was originally thought to be ferric−cupric−peroxide[162] but which was later shown to have a ferryl heme−cupric structure with scission of the original O−O bond.[145] The P_M state is formed spontaneously by decay of the A state under conditions where both the low-spin heme and the Cu_A center are oxidized (the so-called mixed-valence state). This is the state originally described by Chance in low-temperature experiments and called Compound C.[144] The reducing equivalents required to split the O−O bond are taken from the ferrous to ferryl transition of the heme, from the cuprous to cupric transition of Cu_B, and from oxidizing the covalently bonded tyrosine residue to a neutral tyrosyl radical. EPR data (see discussion of the EPR-active P_R state below) using labeled O_2 have identified a fourth OH^- ligand on Cu_B[II]. FTIR data support the notion that the proton of this hydroxide ligand stems from the tyrosine residue, which thus donates both an electron and a proton in the process.[163] The free energy change of the conversion of state A to state P_M is from −3[146] to −4.3[164] kcal/mol based on DFT calculations (see also Figure 8), which is in agreement with the experimental observations that the reaction appears for all practical purposes to go to completion.

The P_R state (Figure 7) is formed from state A under conditions where the enzyme is initially fully reduced, i.e., both Cu_A and heme *a* are reduced upon O_2 binding to heme a_3 (contrast with the P_M state described above). The P_R state has the same optical absorption spectrum as state P_M (Table 2), but the fourth electron required to split the O−O bond now stems from oxidation of heme *a* rather than from oxidation of the tyrosine, which however supplies the necessary proton as indicated by FTIR studies.[163] P_R has an unusual EPR signal (as opposed to P_M which is EPR silent), which arises from Cu_B[II] interacting magnetically with the ferryl heme a_3[66] but which is quenched in P_M presumably due to the additional unpaired spin of the tyrosine radical. The structure of the P_R state is thus established as $Fe[IV]{=}O^{2-}$ $Cu[II]{-}OH^-$ $Tyr\text{-}O^-$. P_R is a unique state of the catalytic cycle also for the reason that it represents the only relatively stable state of the binuclear site that is apparently not charge neutralized according to the principle outlined by Rich.[165] The charge of the porphyrinate dianion of heme a_3 is compensated by the two positive charges of the ferryl iron ($Fe^{4+}{=}O^{2-}$); the Cu_B[II] cation is compensated by the hydroxide ligand and the tyrosinate anion. Propionate D of heme a_3 is charge compensated by making an ion pair to a conserved arginine, but propionate A remains uncompensated so that the overall charge is −1. Calculated this way, all other known intermediates of the catalytic cycle have an overall charge of zero. However, as shown by time-resolved experiments by Belevich et al.[97] (see also refs 93 and 98), the electroneutrality principle of the binuclear center is not violated in the P_R state but the excess negative charge provides the driving force for uptake of a proton to the proton-loading site of the pump mechanism (PLS, see section 7.2).

The F state is formed upon protonation of state P_R (Figure 7). The dramatic difference in the optical absorption spectrum between P_M (or P_R) and F must be due to a change in the absorption spectrum of the heme itself. The OH ligand of Cu_B identified in the P states (see above) is directed toward the axial oxo group of the ferryl heme, and therefore, its protonation to water may be expected to change the axial heme symmetry with a change in the α-band as a result, either due to H bonding from the cupric aquo ligand to the oxo group or, perhaps more likely, due to loss of the resulting water molecule from the coordination sphere of Cu_B. On the other hand, protonation of the tyrosinate close to the heme edge and the heme's hydroxyethyl farnesyl side chain would not be expected to cause such a dramatic change in the optical spectrum. Moreover, several studies have shown that protonation of a state equivalent to P_M (with ferryl heme, cupric copper, and the neutral tyrosine radical) yields a state (called F(dot) or F′) with optical characteristics similar to the F state but without the additional electron.[166] Since protonation of the tyrosine radical is unlikely,[167] these observations independently suggest that it is protonation of the OH^- ligand of Cu_B that changes the P-like heme spectrum to become F like (Table 2). Furthermore, Verkhovsky et al.[168] found that in cytochrome ba_3 from *Th. thermophilus*, which is a type B member of the heme−copper enzyme family,[4] an F-like species is entirely absent from the catalytic reaction sequence. Instead, uptake of the first proton to the binuclear center after the reaction with O_2 (analogous to formation of F) yields a species with optical P-like character. This may hence be a natural example of a case where the proton is taken up into the active site without a spectral shift (from P like to F like), suggesting that the proton acceptor in the catalytic sequence of the ba_3 enzyme is the covalently bonded tyrosinate (known to be present in the *Th. thermophilus* enzyme), in contrast to the OH^- ligand of Cu_B as in the A-type oxidases (however, see ref 169 for a different interpretation).

6.3. O and E States

The BNC in the "as-isolated" cytochrome *c* oxidase is in the so-called O state ("oxidized") with ferric high-spin heme a_3 and cupric Cu_B magnetically coupled so that the EPR characteristics of neither is observed.[141,142] There has been much discussion with regard to the more detailed structure of this state, especially concerning the nature of the bridging ligand between the two metals. "Resting" vs "pulsed" forms as well as "slow" vs fast" have been described (see ref 93 and citations therein). Recent crystallographic work has claimed that the bridge comprises a peroxide molecule,[46,126] which is very difficult to understand in terms of the otherwise quite well understood structures of catalytic cycle intermediates (see ref 93). This is in part augmented by the recent radiation-damage-free structure of B-type oxidase in which the electron density between the two metals has been ascribed to a hydroxide or a water

DOI: 10.1021/acs.chemrev.7b00664
Chem. Rev. 2018, 118, 2469−2490

molecule[170] (see also ref 171). At any rate, it has become clear that state O of the BNC is not a catalytically active state but a relaxed form (or a combination of such forms) generated spontaneously in the absence of electron donors. The bridging ligand in that state could possibly be dioxygen itself or superoxide.[48] Light-triggered electron injection into C*c*O in the O state results in fast reduction of Cu_A and the low-spin heme *a* but no further electron transfer into the binuclear site within several milliseconds.[172] In contrast, when electron injection is performed immediately after reoxidation of C*c*O with O_2, there is electron transfer into the BNC in the submillisecond time domain, and the reaction is accompanied by proton pumping.[172,173] On the basis of such data a catalytically active form of the O state, called O_H, was postulated,[173] different from both pulsed and fast forms described earlier.

O_H was early on suggested to have a hydroxide ligand on heme a_3 (hence the suffix H) based on the resonance Raman work by Rousseau et al.,[174] who identified such a high-spin ferric−OH intermediate with an Fe−O stretching vibration at 450 cm^{-1} (Table 2), which is a very low frequency compared to other ferric heme hydroxide compounds that are usually low spin due to the strong-field hydroxide ligand. Ishigami et al.[175] attribute the low-frequency and the high-spin state to a strong hydrogen bond to the oxygen of the ferric OH^- ligand. Alternatively, it is due to strong bonding of Cu_B to the oxygen atom (see below). It was also predicted[176] that the E_m of the O_H state would have to be much more positive than the redox potentials of ca. 350−400 mV found in anaerobic equilibrium redox titrations of C*c*O.[177] This prediction was fulfilled in the electron injection experiments by Belevich et al.,[178] which showed that injection of a single electron into the O_H state led to exclusive reduction of Cu_B (based on the optical spectral change) with an E_m value at least 120 mV higher than the E_m of the low-spin heme *a*, i.e., >500 mV. It may be of interest to note that on the basis of recent density functional theory (DFT) studies the O_H state is an electronic equilibrium between ferric−OH cupric tyrosinate and cuprous tyrosine radical states.[63,179,180] In both cases the addition of an electron would yield a ferric−OH cuprous tyrosinate state (E_H; Figure 8). Moreover, recent DFT calculations[180] support the prediction[176] that the E_m values of the O_H/E_H and E_H/R redox couples (see Figure 7) are much higher than those obtained in equilibrium redox titrations.

Earlier we proposed based on DFT calculations that one of the key differences between the relaxed O and activated O_H states may be the trigonal planar geometry of the Cu_B center in the latter state.[63] This imparts Cu_B a high operational redox potential and cross-linked Tyr a radical character, whereas in the O state the Cu_B is ligated by three histidine residues, a fourth oxygenous ligand ($-OH^-$), and the tyrosine is anionic. Overall, the conclusion from the study was that the strained BNC structure and a neutral radical on Tyr makes the O_H state kinetically competent in redox-coupled proton pumping in comparison to the O state. In order to model the activated O_H and F_H states, we optimized the geometries by displacing the water near Cu_B to a position such that it does not ligate the copper (see Figure 9). In subsequent studies, Blomberg reached very similar mechanistic conclusions based on DFT calculations performed on larger model systems.[64,180,181] In order to further look into this, we compared the optimized structures of the activated states O_H from these two independent studies.[63,64,180,181] The data in Figure 9 clearly shows that the structure of the active site is very similar in the two cases. Also,

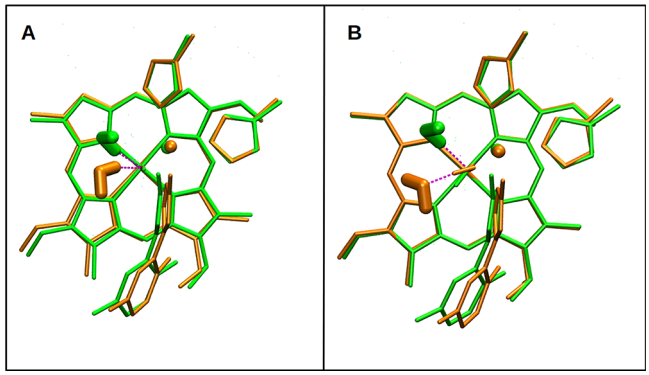

Figure 9. Comparison of structures of the F_H (A) and O_H (B) states from studies by Sharma et al.[63] (orange) and Blomberg[180] (green).

in both studies it was concluded that the structure has the tendency of favoring the cuprous−tyrosine radical electron distribution. Furthermore, using the reported coordinates[180] we calculated the energies of the two structures, which are within 1 kcal/mol from one another.

6.4. Redox Potentials

Figure 7 summarizes the main features of the catalytic cycle and the structures of its intermediates. Originally, the only known redox potentials were those measured by anaerobic redox titrations in which the fully oxidized enzyme was reduced and reoxidized in the presence of suitable redox mediators.[18,141] Briefly, in those titrations the $E_{m,7}$ of Cu_A was found to be ca. 245 mV (n = 1) and almost independent of pH. By contrast, the $E_{m,7}$ values of hemes *a* and a_3 were found to be interdependent presumably due to an electrostatic redox interaction. Thus, the $E_{m,7}$ values of both hemes *a* and a_3 were found to be near 380 mV when the companion heme was oxidized but ca. 230 mV when the companion heme was reduced. The $E_{m,7}$ of Cu_B was estimated to be ca. 390 mV on the basis of appearance of the high-spin ferric EPR signal of heme a_3 at g = 6 upon Cu_B reduction that abolishes the magnetic coupling between them (see ref 93).

Table 3 summarizes the midpoint redox potentials ($E_{m,7}$) of the catalytic cycle intermediates as well as the corresponding standard free energy changes ($-\Delta G_0'$) for each reaction step. Experimental estimates are available only for the P_M/F and F/O_H redox couples; their uncertainty is due to the assumed protonmotive force of 220 mV in well-coupled rat-liver mitochondria supplied with an excess of ATP[176] but is hardly larger than some 20−30 mV. The discrepancy to the free energies calculated by DFT methods (Table 3) is significant especially for the $P_M \rightarrow F$ transition. This transition has a calculated driving force much higher than that of the subsequent $F \rightarrow O_H$ transition, while the experimental estimates for these two reactions are comparable. It should be emphasized that the sum of standard free energies in Table 3 should amount to the $-\Delta G_0'$ of the overall reaction 1, which is 4 × 550 or 2200 meV (see section 2). On this basis and from the experimental estimates of $-\Delta G_0'$ for the $P_M \rightarrow F$ and $F \rightarrow O_H$ steps, the mean values for the $O_H \rightarrow E_H$ and $E_H \rightarrow R$ steps may be estimated (in parentheses, Table 3). Figure 10 shows a plot comparing the $E_{m,7}$ values of the oxidase reaction steps (in red) with the corresponding values of the four one-electron reactions of O_2 reduction to water in aqueous solution[93] (in blue). The figure shows how binding to the enzyme's active site has a remarkable smoothening or leveling effect on the four

DOI: 10.1021/acs.chemrev.7b00664
Chem. Rev. 2018, 118, 2469−2490

Table 3. $E_{m,7}$ Values (mV) and Driving Forces ($-\Delta G_0'$ in meV) in the Catalytic Cycle[a]

	E_m (exp)	$E_{m,7}$ (exp)	$E_{m,7}$ (exp) (pmf = 0)	$-\Delta G_0'$ (exp)	$-\Delta G_0'$ (Kaukonen)	$-\Delta G_0'$ (Blomberg)
$P_M \rightarrow F$	375 (pH 7.7)	417	857	607	798	871
$F \rightarrow O_H$	350 (pH 7.2)	362	802	552	332	477
$O_H \rightarrow E_H$			(660)	(410)	342	277
$E_H \rightarrow R$			(660)	(410)	518	316
$R \rightarrow A$[b]				0	−41	43
$A \rightarrow P_M$[c]				220	124	225

[a] E_m cyt c = 250 mV; E_m O_2/H2O= 800 mV; pmf assumed at 220 mV. Experimental observations from ref 162. Conversion to pH = 7 and pmf = 0 (Wikström and Verkhovsky[176]). Computational data from Kaukonen[146] and Blomberg[180] converted with E_m (cyt c) = 250 mV and E_m (O_2) = 800 mV. Note that the $E_{m,7}$ values for the P_M/F, F/O_H, O_H/E_H, and E_H/R redox transitions are related to the corresponding values of $-\Delta G_0'$ by adding 250 mV (the $E_{m,7}$ of cyt c). The values in parentheses for the $O_H \rightarrow E_H$ and $E_H \rightarrow R$ redox reactions were obtained from the known sum of all of the $-\Delta G_0'$ (exp) values (i.e., 2200 meV), from which the experimental and calculated values of the other transitions were subtracted. The obtained sum of $-\Delta G_0'$ (exp) values for the $O_H \rightarrow E_H$ and $E_H \rightarrow R$ transitions was assumed to be distributed equally between them. [b]These values are based on the equilibrium constant of O_2 binding and differ slightly due to different assumed O_2 activities. [c]This value is obtained from the equilibrium constant as estimated by DFT calculations

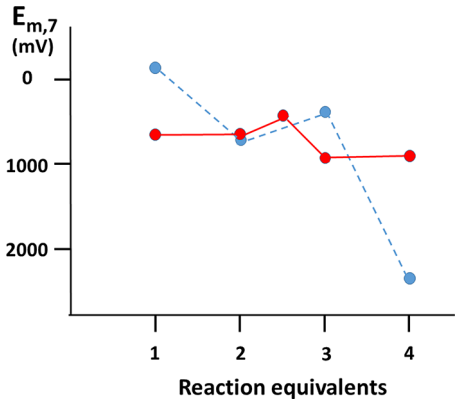

Figure 10. Redox potentials. Redox potentials for the four one-electron reactions reducing O_2 to water are shown in blue for the reaction in aqueous solution[93] and in red for the reactions catalyzed by cytochrome c oxidase (Table 3). Note that the ordinate may also be the standard change in Gibbs free energy ($-\Delta G_0'$, in meV), which is obtained by subtracting 250 mV from the $E_{m,7}$ values plotted. Red point at 2.5 reaction equivalents is not an $E_{m,7}$ value but the combined $-\Delta G_0'$ value for the reactions $R \rightarrow A$ and $A \rightarrow P_M$ to which 250 mV was added (cf. Table 3).

otherwise very different redox potentials. This leveling is, in fact, much more prominent than thought originally[141] for two reasons. First, at that time, the experimental $E_{m,7}$ values of the $P_M \rightarrow F$ and $F \rightarrow O_H$ steps were overestimated due to the erroneous belief that each of these steps would be coupled to pumping of two protons instead of one.[182] Second, at that time it was not realized that the redox potentials measured in anaerobic equilibrium experiments were not relevant for the potentials of the active forms O_H and E_H. At optimum, the leveling of the $E_{m,7}$ values for each of the four one-electron reaction steps should occur at the potential of the $O_2/2H_2O$ redox couple, which is 800 mV in the conditions used here (section 2). As shown in Figure 10, estimates based on currently available experimental data do not deviate much from that optimum. It is also important to realize that the bound dioxygen in state A receives four electrons essentially simultaneously (no experimentally discernible intermediate), so that no "reactive oxygen species" are produced in the reaction.

7. PROTON TRANSLOCATION

7.1. General Principles

The most entertained mechanism of proton translocation by the A-type heme−copper oxidases follows a set of common principles that will be outlined first. The *mechanistic stoichiometry* has been found to be up to one pumped proton per electron transferred from cytochrome c to dioxygen, the electrical charge translocation being equivalent to two charges/e^- due to the uptake of the electrons from the ***P*** side of the membrane and the protons for formation of water ("chemical" protons) from the ***N*** side. Today, these stoichiometric features are well documented in experiments with isolated mitochondria, bacterial cells, and isolated C*c*O from different sources incorporated into phospholipid vesicles.

Wikström and Krab[183] proposed a *directly coupled proton pump* (DCP) principle in which there would be direct electrostatic coupling between the translocated proton and the transferred electron. Such a mechanism would not require large conformational changes or long-range structural interactions. According to this principle, electron transfer would initially be partially compensated for electrostatically by the transfer of a proton originating from the ***N*** side of the membrane to a "pump site" (other subsequent descriptions are "proton trap" and "proton-loading site") located at a short distance from the electron in the BNC in order to enable sufficient Coulombic stabilization by the electron. In the next step, another proton originating from the ***N*** side would arrive at the BNC, completing the oxygen reduction chemistry and annihilating the electron charge. This event would therefore destabilize the proton in the "pump site", lowering its pK_a and thus causing its ejection to the ***P*** side of the membrane. Morgan et al.[184] described this by "*binding of scalar protons to oxygen drives the ejection of the vectorial protons from the pump*". Rich[165] independently arrived at the same principle, based on the electroneutrality concept of the BNC that he had previously established experimentally.[94]

This basic principle of the functioning of the proton pump can be traced back to early proposals where reduction of heme *a* would be coupled to protonation of the PLS (cf. ref 185). The competing view is that electron transfer from heme *a* to the BNC is required to drive the first proton-pumping event, viz. loading of the PLS with a proton. This latter idea was implicit in the mechanistic proposals by Morgan et al.[184] and Rich[165] as well as in the "water-gate" mechanism[116] and the mechanisms proposed by Popovich and Stuchebruchov[186] and

DOI: 10.1021/acs.chemrev.7b00664
Chem. Rev. 2018, 118, 2469−2490

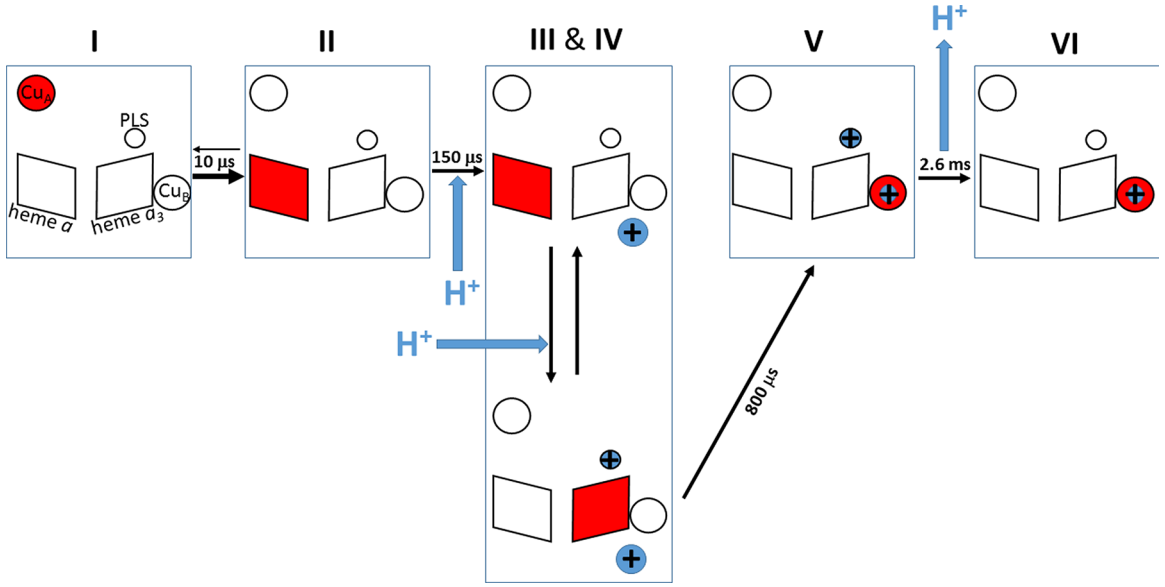

Figure 11. Proton pump mechanism. Mechanism is depicted as revealed from time-resolved electron injection experiments of the $O_H \rightarrow E_H$ transition[172,178] but revised from ref 178 to account for the effect of mutating the K channel lysine, which blocks the 150 μs phase.[98,172] The 150 μs phase includes protonation and movement of lysine-319 closer to the BNC (blue circle below heme a_3), which is necessary to allow electron transfer from heme *a* to heme a_3 and the linked uptake to the PLS of the proton to be pumped (blue circle above heme a_3) in states marked III and IV, respectively. Red color indicates the position of the injected electron.

Siletsky et al.[187] More recent experimental observations have supported this suggestion,[176] because electrometric measurements of charge translocation have shown that the proton movements associated with the proton pump are linked to oxidation of heme *a* by the BNC, not to its reduction by Cu_A (see also Belevich et al.[178]).

All protons to be pumped are taken up from the ***N*** side of the membrane via the so-called D pathway (or D channel) characterized by a conserved aspartate at its opening, an "asparagine gate" domain, a "serine domain", and finally a conserved glutamic acid situated roughly halfway into the membrane dielectric at ca. 10 Å from both heme groups (Figure 5; section 5.3.1). Yoshikawa et al.[47] maintain that in bovine C*c*O all pumped protons are transferred via another pathway, the so-called H channel, and by an indirectly coupled mechanism entirely different from the one discussed in this section (see section 7.4.1).

Several candidates for the "pump site" (PLS) have been proposed. The first one, His-284, one of the ligands of Cu_B, was suggested before the crystal structure was known as part of the so-called histidine cycle mechanism.[184,188] A detail of that mechanism, viz. that proton pumping would be linked only to the reactions of the oxidative phase of the catalytic cycle, was later shown to be erroneous by kinetic experiments, which demonstrated proton pumping coupled to all four one-electron transfers into the BNC.[173] Subsequently, another histidine ligand of Cu_B has been proposed as the PLS,[189] along with the D and A propionates of heme a_3[190−192] and water molecules in their vicinity.[193] Common to all these proposals is the vicinity to the BNC, allowing strong Coulombic proton−electron coupling as required by the DCP principle. A final decision has not been reached, and it is possible that the PLS is not a single binding site but a more poorly defined domain that the proton is occupying, possibly including the propionate A of heme a_3 and water molecules in the vicinity[194] (Figure 5).

7.2. Proton-Pumping Mechanism in Type A Cytochrome *c* Oxidases

Time-resolved dynamic and static equilibrium experiments on type A heme−copper oxidases from both mitochondria and bacteria over a period of nearly four decades have led to the proposal of a general mechanism that follows the directly coupled proton pump principle described above and which conforms to the notion that uptake of the chemical protons is a crucial element of the proton pump. In both these respects it differs fundamentally from alternative mechanisms which will be summarized separately below (section 7.4). The mechanism is proposed to be essentially the same in all four one-electron reaction steps of the catalytic cycle (Figure 7), albeit with some small variations that will be discussed. The mechanistic time frame is largely based on two kinds of time-resolved experiments, either flow-flash data where the reaction is started by photolysis of heme a_3[II]-CO in the presence of O_2 or experiments where a single electron is photoinjected to C*c*O in a defined state, usually O_H. In both cases the progress of electron transfer is usually measured by optical spectroscopy, in some particular studies by resonance Raman and EPR spectroscopy; proton transfer has been measured by electrometry and proton uptake/release by using pH indicators in phospholipid vesicles inlaid with C*c*O. Figure 11 shows this mechanism as applied to the $O_H \rightarrow E_H$ reaction.

Electron transfer from Cu_A to heme *a* is fast (section 5.2) and due to pure quantum-mechanical electron tunneling without linkage to proton movements. However, the redistribution of charge will change the pK_a values of nearby acidic groups, and depending on their location and protonic connectivity and on the pH of the aqueous ***N*** and ***P*** phases, secondary proton movements may occur as seen as a weak pH dependence of the equilibrium $E_{m,7}$ of heme *a*.[94] Reduction of heme *a* may raise the pK_a of the proton-loading site (PLS), but this is insufficient to load the site with a proton from the ***N*** side at pH 7. Loading of the PLS is observed separately, coupled to

DOI: 10.1021/acs.chemrev.7b00664
Chem. Rev. 2018, 118, 2469−2490

the transfer of the electron from heme *a* to the BNC, in time-resolved experiments where the fully reduced enzyme (state R) reacts with O_2.[97] However, such experiments do not distinguish the time sequence of subsequent events of the pump mechanism, which have been addressed by time-resolved electron injection data.

In C*c*O from *P. denitrificans*, single electron injection in the O_H state first leads to ca. 10 μs electron transfer from Cu_A to heme *a* and then to a 150 μs phase of proton uptake from the ***N*** side, which can be attributed to protonation of the PLS.[178] This phase is totally blocked by mutating the key lysine residue in the K pathway to methionine,[172] which supports the notion that electron transfer to heme a_3 in the BNC is actually required for loading the PLS. This observation may, in fact, be an example of the K pathway functioning as a "dielectric well" as proposed by Rich.[106,165] Apparently, the $E_{m,7}$ of heme a_3 is not raised sufficiently by protonation of the PLS relative to the $E_{m,7}$ of heme *a*, so that movement of positive charge closer to heme a_3 by K channel activity is necessary to make the electron transfer to the BNC thermodynamically feasible. An "upswing" of the protonated lysine side chain toward the ***P*** side may be sufficient to achieve this, and such dynamics have been observed in MD simulations.[136] After the 150 μs phase, the injected electron is distributed roughly 60/40 between heme a_3 and heme *a*, which means that even with the PLS protonated and the assistance of the K pathway, the $E_{m,7}$ of heme a_3 is only slightly higher than that of heme *a*. The relatively low $E_{m,7}$ of heme a_3 may be a feature unique for the O_H state and may explain why the electron transfer in this case requires "dielectric assistance" from K channel activity. In contrast, in the A $\rightarrow$ P_R $\rightarrow$ F and subsequent F $\rightarrow$ O_H transitions of the fully reduced enzyme, blockade of the K channel has only a slight effect on the rate.[195] This is possibly attributable to a much higher $E_{m,7}$ of the electron acceptor than is the case in the O_H $\rightarrow$ E_H transition but may nevertheless also be due to an "upflip" of the lysine in this case also.[196]

The 150 μs phase is followed by an 800 μs phase, which is rate limited by net protonation of the BNC via the K pathway.[172,178] This amounts to protonation of the tyrosine and accompanying electron transfer from heme a_3 to Cu_B as verified by optical spectroscopy. Optical spectra reveal that the final destination of the injected electron is indeed Cu_B alone. The lack of any discernible reduction of either heme *a* or a_3 in the final E_H state indicates that the $E_{m,7}$ of Cu_B is at least 120 mV higher than that of the two hemes, implying an $E_{m,7}$ well above 520 mV (assuming that 1% heme *a* reduction would have been detected). This experimental estimate is in good agreement with the $E_{m,7}$ values of the O_H/E_H redox couple of 603 and 528 mV, respectively, obtained from DFT calculations (Table 3).

After the 800 μs phase there is finally a reaction phase with a time constant of ~2.6 ms, which is discernible by the electrometric technique (but not observed by optical spectroscopy), and was interpreted to represent ejection of the proton in the PLS into the aqueous medium on the ***P*** side of the membrane.[178] The driving force for this process is suggested to be the lowered pK_a of the PLS due to neutralization of the BNC by the uptake of the substrate proton. The relatively low rate (compared to a maximum turnover of the *Paracoccus* enzyme of some 1000 s^{-1}) may be due to the special conditions in which only one electron is injected.

Earlier electrometric experiments[172,173] had shown that each of the four one-electron reduction steps in the catalytic cycle (Figure 7) is associated with pumping of one proton across the membrane and with additional uptake of a chemical proton into the binuclear site. In agreement, time-resolved pH indicator data with C*c*O vesicles have demonstrated that one proton is pumped to the ***P*** side in each of the P $\rightarrow$ F and F $\rightarrow$ O_H transitions and that each of these transitions is coupled to uptake of two protons from the aqueous ***N*** side.[197]

7.3. Prevention of Leaks

The prevention of leaks is a fundamental property of a redox-linked proton pump mechanism such as the one briefly outlined above (see refs 190 and 198). For example, electron transfer to the BNC must not be allowed without loading the PLS with a proton. Most of all, primary protonation of the BNC ("chemical proton") linked to the electron transfer must be prevented since, if allowed to occur, the exergonic chemistry driving the endergonic proton pump would be completed without linkage to proton pumping. We note here that Brzezinski et al.[199] proposed an alternative mechanism in which the oxygen reduction chemistry does occur primarily but results in a high-energy conformation of the structure that relaxes secondarily by linkage to proton pumping. This possibility is hard to exclude definitively, but it is made unlikely by both experimental data and conceptual difficulties.[93]

Stimulated by the prediction of water molecules in the hydrophobic cavity between Glu-242 and the hemes, an area that is empty according to the crystal structures, Wikström et al.[116] proposed that such water molecules in a restricted hydrophobic pocket could arrange themselves to catalyze controlled primary proton transfer to the PLS rather than to the BNC, thus securing the first requirement of a functioning redox-linked proton pump. This so-called *water-gated mechanism* has subsequently been criticized[200] but has also gained further support from more sophisticated multiscale approaches[118] as well as from comprehensive molecular dynamics simulations that have included the lipid membrane.[82] Yet, it is evident that this mechanism would not alone be sufficient to prevent proton leaks in the pump mechanism.

Another acute possibility for a leak concerns the situation later on in the mechanistic pump sequence, where the pumped proton has been deposited in the PLS and the chemical proton has been taken up at the BNC, causing a substantial destabilization of the PLS proton (see above). The issue now is how the system prevents the PLS proton from leaking back into the aqueous ***N*** phase, a reaction that is far more favorable thermodynamically than the ejection into the ***P*** phase required for a functioning pump. It is obvious that the gating required here must be of kinetic nature. Blomberg and Siegbahn[198] suggested a positively charged transition state for proton transfer from the ***N*** side to the PLS, which would be stabilized (lowered in energy) by Coulombic interaction with the electron in heme *a* but would be raised in the case where the electron has moved to the BNC, thus preventing back-leak of the proton from the PLS. Another possibility is gating by the position of the side chain of glutamic acid 242 at the end of the D pathway.[122,201] One promising kinetic gate may be provided by the conserved asparagine domain in the D pathway.[109,110] The importance of this latter gate is highlighted by the fact that several mutations in this area cause decoupling of the proton pump without affecting electron transfer.[112,202−205] These gating possibilities have not been quantified in a precise manner, and it remains possible that they all contribute to the high efficiency of proton pumping by the A-type oxidases,

DOI: 10.1021/acs.chemrev.7b00664
Chem. Rev. 2018, 118, 2469−2490

which is not shared by those of type B and C, which lack the D pathway.

7.4. Proposed Alternative Mechanisms

7.4.1. Role of the so-Called H-Channel. Yoshikawa et al.[47,99,206,207] emphasized the importance of the structure that they have called the H channel as the sole transfer path of the pumped protons across the membrane. The H channel is located in subunit I and passes the low-spin heme *a* but is very far away from the binuclear site. Hence, any redox-linked proton coupling involving the H channel would have to be via long-distance interactions, in contrast to the DCP mechanisms described above but in agreement with proposals of indirect conformational coupling by Papa et al.[208] and Rousseau et al.[209]

The H channel structure is not unique for mammalian C*c*O, but most of it is shared by the A-type bacterial heme−copper oxidases (but see below). Extensive mutations in this structure of bacterial C*c*O[104,210] have shown no effects whatsoever on proton pumping and very small perturbations of overall redox activity. This is in complete contrast to results with the mammalian enzyme, published by Yoshikawa et al.,[47] where bovine C*c*O genes were expressed in HeLa cells and three mutations in the H channel structure were reported to abolish proton pumping without effect on electron transfer. Unfortunately, to our knowledge, these results have not been reproduced by other laboratories, and such confirmatory experiments should have very high priority. One reason for this is that if the Yoshikawa mechanism is correct it would have profound evolutionary implications, indicating that the mechanism of proton pumping would be fundamentally different in mammalian (mitochondrial) C*c*O, not only from that of A-type C*c*O in aerobic bacteria despite their very close structural and functional homology but also from yeast mitochondrial C*c*O where mutations in the D and K channels have comparable effects to those in bacterial A-type oxidases and mutations in the H channel are ineffective.[211]

We may analyze the Yoshikawa mechanism by two approaches: one structural and one functional. As already mentioned, the main H channel structures are found also in the bacterial cytochrome *c* oxidases of type A with the exception of the aspartate residue near the ***P*** side of the membrane unique to the vertebral C*c*Os, close to the bimetallic Cu_A center, and a Tyr440-Ser441 motif. In most other respects key hydrophilic residues of the H channel in mammalian C*c*O are conserved in the bacterial A-type C*c*Os. However, all of those hydrophilic H channel residues that were conserved between mammalian and bacterial C*c*Os have been replaced by apolar amino acids in the bacterial quinol oxidases, which are also of type A.[98] Yet, the bacterial A-type quinol oxidases are proton pumps just like their "cousins" in the C*c*O group. Hence, the presence of a H channel structure correlates with the function of the oxidase as a cytochrome *c* oxidase (instead of being a quinol oxidase) but not with the function as a proton pump.

7.4.2. Linkage of the Proton Pump to the Catalytic Cycle. From a functional point of view, Yoshikawa's mechanism defines the steps in the catalytic cycle that are coupled to various aspects of proton transfer, viz. the uptake of the four "chemical" protons to complete the redox chemistry at the BNC, the uptake of protons to be pumped from the ***N*** side into a storage mode near the Mg site, and the release of the stored protons to the aqueous ***P*** side of the membrane. According to the original mechanism by Yoshikawa and colleagues,[212] all four protons to be pumped are taken up from the ***N*** side of the membrane after formation of the R state (see Figure 7) and before this state reacts with O_2 and are deposited in a hydrogen-bonded network around and above heme *a*. In each of the subsequent one-electron transfer reactions of the catalytic cycle (see Figure 7) one proton was proposed to be released to the ***P*** side from this network and one proton taken up to complete the oxygen reduction chemistry at the BNC. However, this scheme is at variance with the time-resolved measurements of proton release and uptake on bacterial enzyme by Brzezinski et al.,[197] who showed that the P → F and F → O transitions are each associated with uptake of *two* protons from the ***N*** side. In a subsequent paper[213] this disparity was realized, the proton-accepting hydrogen-bonded network was revised, and it was proposed instead that each of these two transitions may be associated with uptake of two protons for the O_2 reduction chemistry so that the P → F and F → O reaction steps would *each* be linked to release of 1 proton from the "store" to the P side and to uptake of *two chemical* protons to the BNC. Since each step is also linked to transfer of one electron from cytochrome *c* on the ***P*** side to the BNC, each reaction step is coupled to translocation of two electrical charges across the membrane. This charge translocation stoichiometry is consistent with electrometric data for those reaction steps[98] and also with measurements of the number of protons taken up on the ***N*** side and released on the ***P*** side[197] as well as with the observations of net consumption of about two protons from the medium in the oxidative phase of the catalytic cycle.[94] However, the consumption of *all four chemical protons* in the oxidative phase is very difficult to fit to the structures of the P, F, and O states as they were determined by other data (see section 6 and Figure 7).

This version of the mechanism further suggests that all four protons to be pumped are taken up from the ***N*** phase in a single step following formation of state R and before oxygen binds to form state A. This means altogether that the reaction steps O_H → E and E → R are each associated only with release of one proton from the Mg site to the ***P*** phase, which is in accordance with the observations of release of pumped protons, but incompatible with the observed charge translocation during these two reaction steps. The only charge translocation of each of the O_H → E and E → R steps in the mechanism is electron transfer from cyt *c* to the BNC and release of a proton to the ***P*** side from the PLS, which together amount to less than one electrical charge equivalent across the membrane. In contrast, electrometric experiments on bacterial enzymes have shown that *two* electrical charges cross the membrane in each of these reaction steps, which is consistent with the mechanism discussed earlier (section 7). For these reasons, Yoshikawa's mechanism was recently further revised.[207] In the revised version, each electron transfer to the binuclear center is coupled to uptake of one proton from the ***N*** side of the membrane to the BNC for the chemistry of O_2 reduction, to uptake of one proton from the ***N*** side into a hypothetical "proton pool", and to ejection of one proton from the H-bond network in the Mg domain to the ***P*** side of the membrane. When the "proton pool" is filled with four protons in the R state, they are all transferred to the H-bond network in the Mg domain prior to binding of O_2 to the BNC. As noted by the authors, the distance between the "proton pool" and the H-bond network in the Mg domain must be very small to be consistent with measurements of electrical charge displacement during individual reactions of the catalytic cycle.

DOI: 10.1021/acs.chemrev.7b00664
Chem. Rev. 2018, 118, 2469−2490

With these amendments the new mechanism proposed by Yoshikawa et al.[207] is consistent with time-resolved measurements of electron and charge transfer summarized above (section 7.3). Nevertheless, we find the requirement of two adjacent domains capable of taking up and releasing four protons quite problematic. Moreover, the Mg domain that is particularly important in this alternative model is entirely lacking from the quinol oxidase cytochrome bo_3, which nevertheless belongs to the A class of heme−copper oxidases, lacks the H channel, but is an efficient proton pump.

The four-proton collection mechanism is based on an observed conformational change in helix X of subunit I between the two heme groups that appears to allow protonic contact between the H-bonded network in the Mg domain and the H channel only when the binuclear center is fully reduced and unliganded but which is closed in all other cases.[214] However, these are relatively small changes in a static crystal structure and not unexpected as a result of the fairly large change in valence of heme iron and copper in the BNC. In the absence of dynamic data the link between this change to the mechanism of proton translocation is speculative despite the wide attention that it has received due to the spectacular structural X-ray work of the Yoshikawa group. We also note here that recent atomistic simulations on the entire 13-subunit bovine enzyme and on a smaller core (subunits I−III) do not support a role of the H channel in proton translocation but suggests that it may function as a "dielectric well".[215]

7.4.3. Linkage of the Proton Pump to Oxidoreduction of Heme *a*. Very early on, Artzatbanov et al.[216] proposed a mechanism of proton pumping by cytochrome *c* oxidase where uptake of the pumped proton from the ***N*** side of the membrane is linked to reduction of the low-spin heme *a* and subsequent release of the proton to the aqueous ***P*** side linked to reoxidation of heme *a*. This theme is still maintained in the mechanistic proposals of Papa et al.[208] and Rousseau et al.,[209] but it has been experimentally excluded. As summarized by Siletsky and Konstantinov,[185] the time-resolved measurements of membrane potential show that the main phases of charge separation are linked to oxidation of heme *a* by the BNC, not to its reduction. In fact, in electron injection experiments the relatively small membrane potential generation linked to reduction of heme *a* can be unequivocally attributed to the electrogenic electron transfer from Cu_A to heme *a*.

In two papers published in 2000, Capitanio et al. investigated the release and uptake of redox Bohr protons coupled to oxido−reduction of cytochrome *a* and Cu_A in CO-liganded cytochrome *c* oxidase.[217,218] In the first paper they studied this in the isolated enzyme;[218] in the second paper they used both the isolated enzyme and the oxidase reconstituted in liposomes.[217] They found that a complete redox transition (2 electrons) of cytochrome *a* and Cu_A was linked to uptake or release of 0.4−0.7 protons, as recalculated from Figures 1 and 3 in ref 217. With the single exception of the experiment where cytochrome *a* is initially completely oxidized, $H^+/2e$ values around an average of 0.54 are found (note that this $H^+/2e$ is the sum of the H^+/e of cytochrome *a* and the H^+/e for Cu_A as both participate equally in the redox transitions). This number is intermediate between the values this group had reported earlier (0.65−1.0 $H^+/2e$ for CO-liganded oxidase)[219] and those obtained by Verkhovsky et al. (0.20−0.43).[220]

The present values for the Bohr $H^+/2e$ would imply a 24−41 mV/pH unit dependence of the apparent midpoint potentials, shared between cytochrome *a* and Cu_A. This is not very different from the known slight pH dependences of the midpoint potentials of cytochrome *a* (determined in CO-liganded cytochrome *c* oxidase, a decrease of ca. 10−26 mV/pH unit[221]) and Cu_A (a decrease of 9 mV/pH unit[222]). However, this demonstration of "redox Bohr protons" is certainly not sufficient for postulating that one or both of these two redox centers (cytochrome *a* and Cu_A) are involved in a proton pump. Also, it should be noted that a putative role of a redox reaction in a proton pump does not imply that the stoichiometry of the pump should be reflected in the stoichiometry of Bohr protons observed upon incomplete turnover of the pump mechanism.[183]

In addition to the demonstration of Bohr protons with the isolated enzyme, Capitanio et al. concluded from their experiments with CO-liganded cytochrome *c* oxidase reconstituted in liposomes that upon oxidation of cytochrome *a* and Cu_A these Bohr protons are released at the outside of the vesicles and upon reduction they are taken up from the inside.[217] They conclude this from experiments with these proteoliposomes in the presence of cytochrome *c* and a trace amount of mitochondria providing a way to slowly rereduce the enzyme (with succinate as the source of reducing equivalents) after oxidation with ferricyanide. What they observe measuring pH changes in the medium is (i) fast oxidation of cytochrome *a* with concomitant release of Bohr protons, (ii) slow rereduction with release of scalar succinate protons, and (iii) a pH drift interpreted as equilibration of protons putatively taken up from the inside of the vesicles during phase ii.

This interpretation, if correct, would have a very interesting consequence. Oxidation of cytochrome *a* and Cu_A by ferricyanide probably occurs via cytochrome *c* (see the comparable reduction of cytochrome *a* by ferrocyanide in the absence and presence of cytochrome *c*[223]). Rereduction by succinate catalyzed by the added trace amount of mitochondria will also be mediated by cytochrome *c*. Because electron transfer to the binuclear center is blocked by CO, the output of electrons (to ferricyanide) followed by their return (from succinate) result in proton translocation in this view. Reduction and reoxidation of cytochrome *c* would thus be sufficient for generation of $\Delta\mu_H+$, a genuine *perpetuum mobile*.

8. CONCLUSIONS IN BRIEF

The mechanism of dioxygen activation in cellular respiration is today fairly well established compared to the situation 25 years ago.[141] Major advances include the role of the unique tyrosine residue in the active site that is covalently linked to one of the histidine ligands of Cu_B and which is conserved throughout the superfamily of respiratory heme−copper oxidases. The most recent results suggest that the catalytic importance of this residue considerably exceeds the original idea of assistance in the breaking of the O−O bond[63,180,181] and that it is of key importance in modulating the redox potentials of the catalytic site intermediates. These redox potentials are now established with reasonable accuracy from both experiment and calculations, and the remarkable "leveling effect" by the active site, relative to the potentials of O_2 reduction in solution, is even more dramatic than originally estimated.[141]

The conservation of energy by means of redox-coupled proton pumping in C*c*O is also relatively well understood, at least in the biochemically and biophysically characterized bacterial oxidases of type A but, as we suggest, also in the mitochondrial type A oxidases. In particular, the time-resolved spectroscopic and electrometric approaches have been central

DOI: 10.1021/acs.chemrev.7b00664
Chem. Rev. 2018, 118, 2469−2490

in identifying the order of the electron and proton transfer events during a cycle of the proton pump. The current dominant view is that the proton to be pumped to the ***P*** side of the membrane is transferred to a pump site near the heme a_3 propionates in linkage to each electron transfer from the low-spin heme to the binuclear site and prior to the transfer of the proton to be consumed at that site. The protonation of the binuclear site finally lowers the pK_a of the pump site with expulsion of its proton to the ***P*** side. The latter is not trivial because especially in the presence of a protonmotive force this proton must be prevented from returning to the ***N*** side by kinetic gating processes, some of which are beginning to be revealed not least by computational means. The proton-pumping mechanism seems to be very similar in the four one-electron reactions of the catalytic cycle but with at least one exception. Electron transfer from heme *a* to the binuclear site coupled to proton transfer to the pump site requires charge compensation from partial proton transfer in the K pathway for the case of the $O_H \rightarrow E_H$ transition (and possibly the $E_H \rightarrow R$ step). This is not absolutely mandatory for the $A \rightarrow F$ and $F \rightarrow O_H$ transitions possibly because of the considerably higher redox potentials of the binuclear site (and hence higher driving forces) in these cases (Table 3).

Recent multiscale computational approaches have been beneficial in the modeling and simulation of transient high-energy states, which are difficult to characterize experimentally, thereby providing molecular insights into the available experimental data as well as making new predictions.

AUTHOR INFORMATION

Corresponding Author

*E-mail: marten.wikstrom@helsinki.fi.

ORCID

Mårten Wikström: 0000-0002-7527-4415
Vivek Sharma: 0000-0002-8838-3151

Notes

The authors declare no competing financial interest.

Biographies

Mårten Wikström received his M.D. and Ph.D. degrees at the University of Helsinki in 1971, after which he spent 1 year as a postdoctoral researcher at the University of Amsterdam with Professor E. C. Slater. In 1975−1976 he was Visiting Associate Professor at the University of Pennsylvania with Professor Britton Chance. He worked as an assistant professor at the University of Helsinki until 1983, when he was appointed to a personal Chair in Medical Chemistry (changed to Physical Biochemistry in 2002). In the period 1996−2006 he was Research Professor of the Academy of Finland and from 1998 to 2013 Research Director of the Structural Biology and Biophysics Program of the Institute of Biotechnology. He retired in 2013 but continues as Emeritus Professor. He was the recipient of the Anniversary Prize of the Federation of European Biochemical Societies (FEBS) in 1977, the Scandinavian Anders Jahre Prize in Medicine in 1984 and 1996, and the David Keilin Prize and Medal (British Biochemical Society) in 1997, and he gave the Peter Mitchell Medal Lecture in 2000. He is an elected member of Societas Scientiarum Fennica (1982), the European Molecular Biology Organization (1985), The Royal Swedish Academy of Sciences (chemistry, 1992), and Academia Europaea (2010). His research interests are in molecular bioenergetics, membrane proteins, electron transfer, proton translocation, and mitochondrial diseases

Klaas Krab received his Ph.D. degree at the University of Amsterdam in 1977 in the group of Professor E. C. Slater. Then he spent 2 years as a postdoctoral researcher at the University of Helsinki in the group of Mårten Wikström and 3 years at the Vrije Universiteit Amsterdam in the group of Professor A. H. Stouthamer. From 1983 to his retirement in 2015 he worked first as Assistant Professor and then as Associate Professor in the groups of Professor R. Kraayenhof and Professor H. V. Westerhoff at the same university. Since his retirement he is a guest in the group of Westerhoff.

Vivek Sharma is an Academy of Finland Research Fellow and Principal Investigator at the Department of Physics and also at the Institute of Biotechnology, University of Helsinki. He was earlier an Academy of Finland Postdoctoral Researcher in the group of Professor Ilpo Vattulainen at the Tampere University of Technology, Finland. He completed his doctoral degree in the group of Professor Mårten Wikström. His research interests include determining the molecular mechanism and function of mitochondrial proteins, which he studies with multiscale computational methods.

ACKNOWLEDGMENTS

This work was supported by Societas Scientiarum Fennica (MW), the Magnus Ehrnrooth Foundation (MW, VS), and the Academy of Finland (VS). M.W. is grateful to Jonathan P. Hosler, Peter R. Rich, and Denis L. Rousseau for helpful comments and access to unpublished material. V.S. is thankful to the Center for Scientific Computing, Finland, for computational resources.

REFERENCES

(1) Barber, J. Photosynthetic Generation of Oxygen. *Philos. Trans. R. Soc., B* **2008**, *363*, 2665−2674.
(2) Siegbahn, P. E. Recent Theoretical Studies of Water Oxidation in Photosystem Ii. *J. Photochem. Photobiol., B* **2011**, *104*, 94−99.
(3) Brudvig, G. W. Water Oxidation Chemistry of Photosystem Ii. *Philos. Trans. R. Soc., B* **2008**, *363*, 1211−1219.
(4) Pereira, M. M.; Santana, M.; Teixeira, M. A Novel Scenario for the Evolution of Haem−Copper Oxygen Reductases. *Biochim. Biophys. Acta, Bioenerg.* **2001**, *1505*, 185−208.
(5) Abramson, J.; Riistama, S.; Larsson, G.; Jasaitis, A.; Svensson-Ek, M.; Laakkonen, L.; Puustinen, A.; Iwata, S.; Wikström, M. The Structure of the Ubiquinol Oxidase from Escherichia Coli and Its Ubiquinone Binding Site. *Nat. Struct. Biol.* **2000**, *7*, 910−917.
(6) Thomas, J. W.; Puustinen, A.; Alben, J. O.; Gennis, R. B.; Wikstrom, M. Substitution of Asparagine for Aspartate-135 in Subunit I of the Cytochrome Bo Ubiquinol Oxidase of Escherichia Coli Eliminates Proton-Pumping Activity. *Biochemistry* **1993**, *32*, 10923−10928.
(7) Ma, J.; et al. Glutamate-89 in Subunit Ii of Cytochrome Bo 3 from Escherichia Coli Is Required for the Function of the Heme−Copper Oxidase. *Biochemistry* **1999**, *38*, 15150−15156.
(8) Castresana, J.; Saraste, M. Evolution of Energetic Metabolism: The Respiration-Early Hypothesis. *Trends Biochem. Sci.* **1995**, *20*, 443−448.
(9) Hendriks, J.; Gohlke, U.; Saraste, M. From No to Oo: Nitric Oxide and Dioxygen in Bacterial Respiration. *J. Bioenerg. Biomembr.* **1998**, *30*, 15−24.
(10) Mitchell, P. Coupling of Phosphorylation to Electron and Hydrogen Transfer by a Chemi-Osmotic Type of Mechanism. *Nature* **1961**, *191*, 144−148.
(11) Wikstrom, M. K. Proton Pump Coupled to Cytochrome C Oxidase in Mitochondria. *Nature* **1977**, *266*, 271−273.
(12) Kim, Y. C.; Wikström, M.; Hummer, G. Kinetic Models of Redox-Coupled Proton Pumping. *Proc. Natl. Acad. Sci. U. S. A.* **2007**, *104*, 2169−2174.

DOI: 10.1021/acs.chemrev.7b00664
Chem. Rev. 2018, 118, 2469−2490

(13) Rauhamäki, V.; Wikström, M. The Causes of Reduced Proton-Pumping Efficiency in Type B and C Respiratory Heme-Copper Oxidases, and in Some Mutated Variants of Type A. *Biochim. Biophys. Acta, Bioenerg.* **2014**, *1837*, 999−1003.
(14) Han, H.; Hemp, J.; Pace, L. A.; Ouyang, H.; Ganesan, K.; Roh, J. H.; Daldal, F.; Blanke, S. R.; Gennis, R. B. Adaptation of Aerobic Respiration to Low O2 Environments. *Proc. Natl. Acad. Sci. U. S. A.* **2011**, *108*, 14109−14114.
(15) Hendriks, J. H.; Jasaitis, A.; Saraste, M.; Verkhovsky, M. I. Proton and Electron Pathways in the Bacterial Nitric Oxide Reductase†,⊥. *Biochemistry* **2002**, *41*, 2331−2340.
(16) Watmough, N. J.; Field, S. J.; Hughes, R. J.; Richardson, D. J. *The Bacterial Respiratory Nitric Oxide Reductase*; Portland Press Ltd.: London, UK, 2009.
(17) Humphrey, W.; Dalke, A.; Schulten, K. Vmd: Visual Molecular Dynamics. *J. Mol. Graphics* **1996**, *14*, 33−38.
(18) Dutton, P. L.; Wilson, D. F.; Lee, C.-P. Oxidation-Reduction Potentials of Cytochromes in Mitochondria. *Biochemistry* **1970**, *9*, 5077−5082.
(19) Ndubuizu, O.; LaManna, J. C. Brain Tissue Oxygen Concentration Measurements. *Antioxid. Redox Signaling* **2007**, *9*, 1207−1220.
(20) Hinkle, P. C. P/O Ratios of Mitochondrial Oxidative Phosphorylation. *Biochim. Biophys. Acta, Bioenerg.* **2005**, *1706*, 1−11.
(21) Chamalaun, R.; Tager, J. Stoicheiometry of Oxidative Phosphorylation with Tetramethyl-P-Phenylenediamine in Rat-Liver Mitochondria. *Biochim. Biophys. Acta, Bioenerg.* **1969**, *180*, 204−206.
(22) Watt, I. N.; Montgomery, M. G.; Runswick, M. J.; Leslie, A. G.; Walker, J. E. Bioenergetic Cost of Making an Adenosine Triphosphate Molecule in Animal Mitochondria. *Proc. Natl. Acad. Sci. U. S. A.* **2010**, *107*, 16823−16827.
(23) Wikström, M.; Hummer, G. Stoichiometry of Proton Translocation by Respiratory Complex I and Its Mechanistic Implications. *Proc. Natl. Acad. Sci. U. S. A.* **2012**, *109*, 4431−4436.
(24) Ludwig, B.; Bender, E.; Arnold, S.; Hüttemann, M.; Lee, I.; Kadenbach, B. Cytochrome C Oxidase and the Regulation of Oxidative Phosphorylation. *ChemBioChem* **2001**, *2*, 392−403.
(25) Kadenbach, B.; Hüttemann, M. The Subunit Composition and Function of Mammalian Cytochrome C Oxidase. *Mitochondrion* **2015**, *24*, 64−76.
(26) Tsukihara, T.; Aoyama, H.; Yamashita, E.; Tomizaki, T.; Yamaguchi, H.; Shinzawa-Itoh, K.; Nakashima, R.; Yaono, R.; Yoshikawa, S. The Whole Structure of the 13-Subunit Oxidized Cytochrome C Oxidase at 2.8 Å. *Science* **1996**, *272*, 1136−1144.
(27) Sharma, V.; Puustinen, A.; Wikström, M.; Laakkonen, L. Sequence Analysis of the Cbb 3 Oxidases and an Atomic Model for the Rhodobacter Sphaeroides Enzyme. *Biochemistry* **2006**, *45*, 5754−5765.
(28) Tomson, F. L.; Morgan, J. E.; Gu, G.; Barquera, B.; Vygodina, T.; Gennis, R. B. Substitutions for Glutamate 101 in Subunit Ii of Cytochrome C Oxidase from Rhodobacter Sphaeroides Result in Blocking the Proton-Conducting K-Channel. *Biochemistry* **2003**, *42*, 1711−1717.
(29) Brändén, M.; Tomson, F.; Gennis, R. B.; Brzezinski, P. The Entry Point of the K-Proton-Transfer Pathway in Cytochrome C Oxidase. *Biochemistry* **2002**, *41*, 10794−10798.
(30) Haltia, T.; Saraste, M.; Wikström, M. Subunit III of Cytochrome C Oxidase Is Not Involved in Proton Translocation: A Site-Directed Mutagenesis Study. *EMBO J.* **1991**, *10*, 2015.
(31) Bratton, M. R.; Pressler, M. A.; Hosler, J. P. Suicide Inactivation of Cytochrome C Oxidase: Catalytic Turnover in the Absence of Subunit Iii Alters the Active Site. *Biochemistry* **1999**, *38*, 16236−16245.
(32) Gilderson, G.; Salomonsson, L.; Aagaard, A.; Gray, J.; Brzezinski, P.; Hosler, J. Subunit III of Cytochrome C Oxidase of Rhodobacter Sphaeroides Is Required to Maintain Rapid Proton Uptake through the D Pathway at Physiologic pH. *Biochemistry* **2003**, *42*, 7400−7409.
(33) Hosler, J. P. The Influence of Subunit III of Cytochrome C Oxidase on the D Pathway, the Proton Exit Pathway and Mechanism-Based Inactivation in Subunit I. *Biochim. Biophys. Acta, Bioenerg.* **2004**, *1655*, 332−339.
(34) Riistama, S.; Puustinen, A.; García-Horsman, A.; Iwata, S.; Michel, H.; Wikström, M. Channelling of Dioxygen into the Respiratory Enzyme. *Biochim. Biophys. Acta, Bioenerg.* **1996**, *1275*, 1−4.
(35) Sharma, V.; Ala-Vannesluoma, P.; Vattulainen, I.; Wikström, M.; Róg, T. Role of Subunit III and Its Lipids in the Molecular Mechanism of Cytochrome C Oxidase. *Biochim. Biophys. Acta, Bioenerg.* **2015**, *1847*, 690−697.
(36) Qian, J.; et al. Role of the Conserved Arginine Pair in Proton and Electron Transfer in Cytochrome C Oxidase. *Biochemistry* **2004**, *43*, 5748−5756.
(37) Wikström, M.; Ribacka, C.; Molin, M.; Laakkonen, L.; Verkhovsky, M.; Puustinen, A. Gating of Proton and Water Transfer in the Respiratory Enzyme Cytochrome C Oxidase. *Proc. Natl. Acad. Sci. U. S. A.* **2005**, *102*, 10478−10481.
(38) Ribacka, C.; Verkhovsky, M. I.; Belevich, I.; Bloch, D. A.; Puustinen, A.; Wikström, M. An Elementary Reaction Step of the Proton Pump Is Revealed by Mutation of Tryptophan-164 to Phenylalanine in Cytochrome C Oxidase from Paracoccus Denitrificans. *Biochemistry* **2005**, *44*, 16502−16512.
(39) Mills, D. A.; Geren, L.; Hiser, C.; Schmidt, B.; Durham, B.; Millett, F.; Ferguson-Miller, S. An Arginine to Lysine Mutation in the Vicinity of the Heme Propionates Affects the Redox Potentials of the Hemes and Associated Electron and Proton Transfer in Cytochrome C Oxidase. *Biochemistry* **2005**, *44*, 10457−10465.
(40) von Ballmoos, C.; Gonska, N.; Lachmann, P.; Gennis, R. B.; Ädelroth, P.; Brzezinski, P. Mutation of a Single Residue in the Ba3 Oxidase Specifically Impairs Protonation of the Pump Site. *Proc. Natl. Acad. Sci. U. S. A.* **2015**, *112*, 3397−3402.
(41) Tsukihara, T.; Aoyama, H.; Yamashita, E.; Tomizaki, T.; Yamaguchi, H.; Shinzawa-Itoh, K.; Nakashima, R.; Yaono, R.; Yoshikawa, S. Structures of Metal Sites of Oxidized Bovine Heart Cytochrome C Oxidase at 2.8 A. *Science* **1995**, *269*, 1069−1074.
(42) Yoshikawa, S.; et al. Redox-Coupled Crystal Structural Changes in Bovine Heart Cytochrome C Oxidase. *Science* **1998**, *280*, 1723−1729.
(43) Qin, L.; Hiser, C.; Mulichak, A.; Garavito, R. M.; Ferguson-Miller, S. Identification of Conserved Lipid/Detergent-Binding Sites in a High-Resolution Structure of the Membrane Protein Cytochrome C Oxidase. *Proc. Natl. Acad. Sci. U. S. A.* **2006**, *103*, 16117−16122.
(44) Qin, L.; Liu, J.; Mills, D. A.; Proshlyakov, D. A.; Hiser, C.; Ferguson-Miller, S. Redox-Dependent Conformational Changes in Cytochrome C Oxidase Suggest a Gating Mechanism for Proton Uptake. *Biochemistry* **2009**, *48*, 5121−5130.
(45) Bhagi-Damodaran, A.; et al. Why Copper Is Preferred over Iron for Oxygen Activation and Reduction in Haem-Copper Oxidases. *Nat. Chem.* **2017**, *9*, 257−263.
(46) Aoyama, H.; Muramoto, K.; Shinzawa-Itoh, K.; Hirata, K.; Yamashita, E.; Tsukihara, T.; Ogura, T.; Yoshikawa, S. A Peroxide Bridge between Fe and Cu Ions in the O_2 Reduction Site of Fully Oxidized Cytochrome C Oxidase Could Suppress the Proton Pump. *Proc. Natl. Acad. Sci. U. S. A.* **2009**, *106*, 2165−2169.
(47) Yoshikawa, S.; Shimada, A. Reaction Mechanism of Cytochrome C Oxidase. Chem. *Chem. Rev.* **2015**, *115*, 1936−1989.
(48) Kaila, V. R.; Oksanen, E.; Goldman, A.; Bloch, D. A.; Verkhovsky, M. I.; Sundholm, D.; Wikström, M. A Combined Quantum Chemical and Crystallographic Study on the Oxidized Binuclear Center of Cytochrome C Oxidase. *Biochim. Biophys. Acta, Bioenerg.* **2011**, *1807*, 769−778.
(49) Buschmann, S.; Warkentin, E.; Xie, H.; Langer, J. D.; Ermler, U.; Michel, H. The Structure of Cbb3 Cytochrome Oxidase Provides Insights into Proton Pumping. *Science* **2010**, *329*, 327−330.
(50) Hemp, J.; Christian, C.; Barquera, B.; Gennis, R. B.; Martínez, T. J. Helix Switching of a Key Active-Site Residue in the Cytochrome Cbb 3 Oxidases. *Biochemistry* **2005**, *44*, 10766−10775.
(51) Hemp, J.; Robinson, D. E.; Ganesan, K. B.; Martinez, T. J.; Kelleher, N. L.; Gennis, R. B. Evolutionary Migration of a Post-

DOI: 10.1021/acs.chemrev.7b00664
Chem. Rev. 2018, 118, 2469−2490

Translationally Modified Active-Site Residue in the Proton-Pumping Heme-Copper Oxygen Reductases. *Biochemistry* **2006**, *45*, 15405−15410.
(52) Rauhamäki, V.; Baumann, M.; Soliymani, R.; Puustinen, A.; Wikström, M. Identification of a Histidine-Tyrosine Cross-Link in the Active Site of the Cbb3-Type Cytochrome C Oxidase from Rhodobacter Sphaeroides. *Proc. Natl. Acad. Sci. U. S. A.* **2006**, *103*, 16135−16140.
(53) Sharma, V.; Wikström, M.; Kaila, V. R. Stabilization of the Peroxy Intermediate in the Oxygen Splitting Reaction of Cytochrome Cbb 3. *Biochim. Biophys. Acta, Bioenerg.* **2011**, *1807*, 813−818.
(54) Hino, T.; Matsumoto, Y.; Nagano, S.; Sugimoto, H.; Fukumori, Y.; Murata, T.; Iwata, S.; Shiro, Y. Structural Basis of Biological N2o Generation by Bacterial Nitric Oxide Reductase. *Science* **2010**, *330*, 1666−1670.
(55) Matsumoto, Y.; Tosha, T.; Pisliakov, A. V.; Hino, T.; Sugimoto, H.; Nagano, S.; Sugita, Y.; Shiro, Y. Crystal Structure of Quinol-Dependent Nitric Oxide Reductase from Geobacillus Stearothermophilus. *Nat. Struct. Mol. Biol.* **2012**, *19*, 238−245.
(56) Hino, T.; Nagano, S.; Sugimoto, H.; Tosha, T.; Shiro, Y. Molecular Structure and Function of Bacterial Nitric Oxide Reductase. *Biochim. Biophys. Acta, Bioenerg.* **2012**, *1817*, 680−687.
(57) ter Beek, J.; Krause, N.; Ädelroth, P. Investigating the Proton Donor in the NO Reductase from Paracoccus denitrificans. *PLoS One* **2016**, *11*, e0152745.
(58) Blomberg, M. R.; Ädelroth, P. The Mechanism for Oxygen Reduction in Cytochrome C Dependent Nitric Oxide Reductase (Cnor) as Obtained from a Combination of Theoretical and Experimental Results. *Biochim. Biophys. Acta, Bioenerg.* **2017**, *1858*, 884−894.
(59) Collman, J. P.; Devaraj, N. K.; Decréau, R. A.; Yang, Y.; Yan, Y.-L.; Ebina, W.; Eberspacher, T. A.; Chidsey, C. E. A Cytochrome C Oxidase Model Catalyzes Oxygen to Water Reduction under Rate-Limiting Electron Flux. *Science* **2007**, *315*, 1565−1568.
(60) Kim, E.; Chufán, E. E.; Kamaraj, K.; Karlin, K. D. Synthetic Models for Heme− Copper Oxidases. *Chem. Rev.* **2004**, *104*, 1077−1134.
(61) Nanthakumar, A.; et al. Oxo-and Hydroxo-Bridged (Porphyrin) Iron (Iii)-Copper (Ii) Species as Cytochrome C Oxidase Models: Acid-Base Interconversions and X-Ray Structure of the Fe (Iii)-(O2-)-Cu (Ii) Complex. *J. Am. Chem. Soc.* **1993**, *115*, 8513−8514.
(62) Karlin, K. D.; Nanthakumar, A.; Fox, S.; Murthy, N. N.; Ravi, N.; Huynh, B. H.; Orosz, R. D.; Day, E. P. X-Ray Structure and Physical-Properties of the Oxo-Bridged Complex ((F-8-Tpp) Fe-O-Cu (Tmpa))(+), F-8-Tpp Equals Tetrakis (2, 6-Difluorophenyl) Porphyrinate (2-), Tmpa Equals Tris (2-Pyridylmethyl) Amine-Modeling the Cytochrome-C-Oxidase Fe-Cu Heterodinuclear Active-Site. *J. Am. Chem. Soc.* **1994**, *116*, 4753−4763.
(63) Sharma, V.; Karlin, K. D.; Wikström, M. Computational Study of the Activated Oh State in the Catalytic Mechanism of Cytochrome C Oxidase. *Proc. Natl. Acad. Sci. U. S. A.* **2013**, *110*, 16844−16849.
(64) Blomberg, M. R.; Siegbahn, P. E. How Cytochrome c Oxidase Can Pump Four Protons Per Oxygen Molecule at High Electrochemical Gradient. *Biochim. Biophys. Acta, Bioenerg.* **2015**, *1847*, 364−376.
(65) Han Du, W.-G.; Noodleman, L. Broken Symmetry DFT Calculations/Analysis for Oxidized and Reduced Dinuclear Center in Cytochrome C Oxidase: Relating Structures, Protonation States, Energies, and Mössbauer Properties in ba3 Thermus thermophilus. *Inorg. Chem.* **2015**, *54*, 7272.
(66) Morgan, J. E.; Verkhovsky, M. I.; Palmer, G.; Wikström, M. Role of the Pr Intermediate in the Reaction of Cytochrome C Oxidase with O2. *Biochemistry* **2001**, *40*, 6882−6892.
(67) Poiana, F.; von Ballmoos, C.; Gonska, N.; Blomberg, M. R.; Ädelroth, P.; Brzezinski, P. Splitting of the O−O Bond at the Heme-Copper Catalytic Site of Respiratory Oxidases. *Sci. Adv.* **2017**, *3*, e1700279.
(68) Blomberg, M. R.; Siegbahn, P. E.; Wikström, M. Metal-Bridging Mechanism for O− O Bond Cleavage in Cytochrome C Oxidase. *Inorg. Chem.* **2003**, *42*, 5231−5243.
(69) Hematian, S.; Garcia-Bosch, I.; Karlin, K. D. Synthetic Heme/Copper Assemblies: Toward an Understanding of Cytochrome C Oxidase Interactions with Dioxygen and Nitrogen Oxides. *Acc. Chem. Res.* **2015**, *48*, 2462−2474.
(70) Chatterjee, S.; Sengupta, K.; Hematian, S.; Karlin, K. D.; Dey, A. Electrocatalytic O2-Reduction by Synthetic Cytochrome C Oxidase Mimics: Identification of a "Bridging Peroxo" Intermediate Involved in Facile 4e−/4h+ O2-Reduction. *J. Am. Chem. Soc.* **2015**, *137*, 12897−12905.
(71) Adam, S. M.; Garcia-Bosch, I.; Schaefer, A. W.; Sharma, S. K.; Siegler, M. A.; Solomon, E. I.; Karlin, K. D. Critical Aspects of Heme−Peroxo−Cu Complex Structure and Nature of Proton Source Dictate Metal−Operoxo Breakage Versus Reductive O−O Cleavage Chemistry. *J. Am. Chem. Soc.* **2017**, *139*, 472−481.
(72) Schaefer, A. W.; Kieber-Emmons, M. T.; Adam, S. M.; Karlin, K. D.; Solomon, E. I. Phenol-Induced O−O Bond Cleavage in a Low-Spin Heme-Peroxo-Copper Complex: Implications for O2 Reduction in Heme-Copper Oxidases. *J. Am. Chem. Soc.* **2017**, *139*, 7958−7973.
(73) Yoshioka, Y.; Kawai, H.; Yamaguchi, K. Theoretical Study of Role of H 2 O Molecule on Initial Stage of Reduction of O_2 Molecule in Active Site of Cytochrome C Oxidase. *Chem. Phys. Lett.* **2003**, *374*, 45−52.
(74) Al-Abdul-Wahid, M. S.; Evanics, F.; Prosser, R. S. Dioxygen Transmembrane Distributions and Partitioning Thermodynamics in Lipid Bilayers and Micelles. *Biochemistry* **2011**, *50*, 3975−3983.
(75) Möller, M. N.; Li, Q.; Chinnaraj, M.; Cheung, H. C.; Lancaster, J. R., Jr; Denicola, A. Solubility and Diffusion of Oxygen in Phospholipid Membranes. *Biochim. Biophys. Acta, Biomembr.* **2016**, *1858*, 2923−2930.
(76) Cordeiro, R. M. Reactive Oxygen Species at Phospholipid Bilayers: Distribution, Mobility and Permeation. *Biochim. Biophys. Acta, Biomembr.* **2014**, *1838*, 438−444.
(77) Shinzawa-Itoh, K.; et al. Structures and Physiological Roles of 13 Integral Lipids of Bovine Heart Cytochrome *c* Oxidase. *EMBO J.* **2007**, *26*, 1713−1725.
(78) Svensson-Ek, M.; Abramson, J.; Larsson, G.; Törnroth, S.; Brzezinski, P.; Iwata, S. The X-Ray Crystal Structures of Wild-Type and Eq (I-286) Mutant Cytochrome C Oxidases from Rhodobacter Sphaeroides. *J. Mol. Biol.* **2002**, *321*, 329−339.
(79) Luna, V. M.; Chen, Y.; Fee, J. A.; Stout, C. D. Crystallographic Studies of Xe and Kr Binding within the Large Internal Cavity of Cytochrome Ba 3 from Thermus Thermophilus: Structural Analysis and Role of Oxygen Transport Channels in the Heme− Cu Oxidases. *Biochemistry* **2008**, *47*, 4657−4665.
(80) Luna, V. M.; Fee, J. A.; Deniz, A. A.; Stout, C. D. Mobility of Xe Atoms within the Oxygen Diffusion Channel of Cytochrome Ba 3 Oxidase. *Biochemistry* **2012**, *51*, 4669−4676.
(81) Schmidt, B.; McCracken, J.; Ferguson-Miller, S. A Discrete Water Exit Pathway in the Membrane Protein Cytochrome C Oxidase. *Proc. Natl. Acad. Sci. U. S. A.* **2003**, *100*, 15539−15542.
(82) Sharma, V.; Enkavi, G.; Vattulainen, I.; Róg, T.; Wikström, M. Proton-Coupled Electron Transfer and the Role of Water Molecules in Proton Pumping by Cytochrome C Oxidase. *Proc. Natl. Acad. Sci. U. S. A.* **2015**, *112*, 2040−2045.
(83) Moser, C. C.; Farid, T. A.; Chobot, S. E.; Dutton, P. L. Electron Tunneling Chains of Mitochondria. *Biochim. Biophys. Acta, Bioenerg.* **2006**, *1757*, 1096−1109.
(84) Blumberger, J. Recent Advances in the Theory and Molecular Simulation of Biological Electron Transfer Reactions. *Chem. Rev.* **2015**, *115*, 11191−11238.
(85) Moser, C. C.; Keske, J. M.; Warncke, K.; Farid, R. S.; Dutton, P. L. Nature of Biological Electron Transfer. *Nature* **1992**, *355*, 796.
(86) Winkler, J. R.; Gray, H. B. Electron Flow through Metalloproteins. *Chem. Rev.* **2014**, *114*, 3369.

DOI: 10.1021/acs.chemrev.7b00664
Chem. Rev. 2018, 118, 2469−2490

(87) Tan, M.-L.; Balabin, I.; Onuchic, J. N. Dynamics of Electron Transfer Pathways in Cytochrome c Oxidase. *Biophys. J.* **2004**, *86*, 1813−1819.
(88) Shimada, S.; et al. Complex Structure of Cytochrome *c*−Cytochrome *c* oxidase Reveals a Novel Protein−Protein Interaction Mode. *EMBO J.* **2017**, *36*, 291−300.
(89) Witt, H.; Malatesta, F.; Nicoletti, F.; Brunori, M.; Ludwig, B. Tryptophan 121 of Subunit Ii Is the Electron Entry Site to Cytochrome-C Oxidase in Paracoccus Denitrificans Involvement of a Hydrophobic Patch in the Docking Reaction. *J. Biol. Chem.* **1998**, *273*, 5132−5136.
(90) Witt, H.; Malatesta, F.; Nicoletti, F.; Brunori, M.; Ludwig, B. Cytochrome-C− Binding Site on Cytochrome Oxidase in Paracoccus Denitrificans. *Eur. J. Biochem.* **1998**, *251*, 367−373.
(91) Flöck, D.; Helms, V. Protein−Protein Docking of Electron Transfer Complexes: Cytochrome C Oxidase and Cytochrome C. *Proteins: Struct., Funct., Genet.* **2002**, *47*, 75−85.
(92) Lyons, J. A.; Nissen, P. Brief Encounters of Cytochrome C. *EMBO J.* **2017**, *36*, 250−251.
(93) Kaila, V. R.; Verkhovsky, M. I.; Wikström, M. Wikström, M. Proton-Coupled Electron Transfer in Cytochrome Oxidase. *Chem. Rev.* **2010**, *110*, 7062−7081.
(94) Mitchell, R.; Rich, P. R. Proton Uptake by Cytochrome C Oxidase on Reduction and on Ligand Binding. *Biochim. Biophys. Acta, Bioenerg.* **1994**, *1186*, 19−26.
(95) Verkhovsky, M. I.; Jasaitis, A.; Wikström, M. Ultrafast Haem−Haem Electron Transfer in Cytochrome C Oxidase. *Biochim. Biophys. Acta, Bioenerg.* **2001**, *1506*, 143−146.
(96) Jasaitis, A.; Johansson, M. P.; Wikström, M.; Vos, M. H.; Verkhovsky, M. I. Nanosecond Electron Tunneling between the Hemes in Cytochrome Bo3. *Proc. Natl. Acad. Sci. U. S. A.* **2007**, *104*, 20811−20814.
(97) Belevich, I.; Verkhovsky, M. I.; Wikström, M. Proton-Coupled Electron Transfer Drives the Proton Pump of Cytochrome C Oxidase. *Nature* **2006**, *440*, 829−832.
(98) Wikström, M.; Sharma, V.; Kaila, V. R.; Hosler, J. P.; Hummer, G. New Perspectives on Proton Pumping in Cellular Respiration. Chem. *Chem. Rev.* **2015**, *115*, 2196−2221.
(99) Tsukihara, T.; et al. The Low-Spin Heme of Cytochrome C Oxidase as the Driving Element of the Proton-Pumping Process. *Proc. Natl. Acad. Sci. U. S. A.* **2003**, *100*, 15304−15309.
(100) Umena, Y.; Kawakami, K.; Shen, J.-R.; Kamiya, N. Crystal Structure of Oxygen-Evolving Photosystem Ii at a Resolution of 1.9 Å. *Nature* **2011**, *473*, 55−60.
(101) Fetter, J. R.; et al. Possible Proton Relay Pathways in Cytochrome C Oxidase. *Proc. Natl. Acad. Sci. U. S. A.* **1995**, *92*, 1604−1608.
(102) Hosler, J. P.; et al. Polar Residues in Helix Viii of Subunit I of Cytochrome C Oxidase Influence the Activity and the Structure of the Active Site. *Biochemistry* **1996**, *35*, 10776−10783.
(103) Konstantinov, A. A.; Siletsky, S.; Mitchell, D.; Kaulen, A.; Gennis, R. B. The Roles of the Two Proton Input Channels in Cytochrome C Oxidase from Rhodobacter Sphaeroides Probed by the Effects of Site-Directed Mutations on Time-Resolved Electrogenic Intraprotein Proton Transfer. *Proc. Natl. Acad. Sci. U. S. A.* **1997**, *94*, 9085−9090.
(104) Lee, H.-m.; Das, T. K.; Rousseau, D. L.; Mills, D.; Ferguson-Miller, S.; Gennis, R. B. Mutations in the Putative H-Channel in the Cytochrome C Oxidase from Rhodobacter Sphaeroides Show That This Channel Is Not Important for Proton Conduction but Reveal Modulation of the Properties of Heme A. *Biochemistry* **2000**, *39*, 2989−2996.
(105) Wikström, M.; Jasaitis, A.; Backgren, C.; Puustinen, A.; Verkhovsky, M. I. The Role of the D-and K-Pathways of Proton Transfer in the Function of the Haem−Copper Oxidases. *Biochim. Biophys. Acta, Bioenerg.* **2000**, *1459*, 514−520.
(106) Jünemann, S.; Meunier, B.; Gennis, R. B.; Rich, P. R. Effects of Mutation of the Conserved Lysine-362 in Cytochrome C Oxidase from Rhodobacter Sphaeroides. *Biochemistry* **1997**, *36*, 14456−14464.
(107) Rich, P. R.; Maréchal, A. Functions of the Hydrophilic Channels in Protonmotive Cytochrome C Oxidase. *J. R. Soc., Interface* **2013**, *10*, 20130183.
(108) Agmon, N. The Grotthuss Mechanism. *Chem. Phys. Lett.* **1995**, *244*, 456−462.
(109) Henry, R. M.; Yu, C.-H.; Rodinger, T.; Pomès, R. Functional Hydration and Conformational Gating of Proton Uptake in Cytochrome C Oxidase. *J. Mol. Biol.* **2009**, *387*, 1165−1185.
(110) Liang, R.; Swanson, J. M.; Wikström, M.; Voth, G. A. Understanding the Essential Proton-Pumping Kinetic Gates and Decoupling Mutations in Cytochrome C Oxidase. *Proc. Natl. Acad. Sci. U. S. A.* **2017**, *114*, 5924−5929.
(111) Han, D.; Namslauer, A.; Pawate, A.; Morgan, J. E.; Nagy, S.; Vakkasoglu, A. S.; Brzezinski, P.; Gennis, R. B. Replacing Asn207 by Aspartate at the Neck of the D Channel in the Aa3-Type Cytochrome C Oxidase from Rhodobacter Sphaeroides Results in Decoupling the Proton Pump. *Biochemistry* **2006**, *45*, 14064−14074.
(112) Pfitzner, U.; Hoffmeier, K.; Harrenga, A.; Kannt, A.; Michel, H.; Bamberg, E.; Richter, O.-M.; Ludwig, B. Tracing the D-Pathway in Reconstituted Site-Directed Mutants of Cytochrome C Oxidase from Paracoccus Denitrificans. *Biochemistry* **2000**, *39*, 6756−6762.
(113) Siegbahn, P. E. M.; Blomberg, M. R. A. Mutations in the D-Channel of Cytochrome C Oxidase Causes Leakage of the Proton Pump. *FEBS Lett.* **2014**, *588*, 545−548.
(114) Pomès, R.; Hummer, G.; Wikström, M. Structure and Dynamics of a Proton Shuttle in Cytochrome C Oxidase. *Biochim. Biophys. Acta, Bioenerg.* **1998**, *1365*, 255−260.
(115) Hofacker, I.; Schulten, K. Oxygen and Proton Pathways in Cytochrome C Oxidase. *Proteins: Struct., Funct., Genet.* **1998**, *30*, 100−107.
(116) Wikström, M.; Verkhovsky, M. I.; Hummer, G. Water-Gated Mechanism of Proton Translocation by Cytochrome C Oxidase. *Biochim. Biophys. Acta, Bioenerg.* **2003**, *1604*, 61−65.
(117) Zheng, X.; Medvedev, D. M.; Swanson, J.; Stuchebrukhov, A. A. Computer Simulation of Water in Cytochrome C Oxidase. *Biochim. Biophys. Acta, Bioenerg.* **2003**, *1557*, 99−107.
(118) Liang, R.; Swanson, J. M. J.; Peng, Y.; Wikström, M.; Voth, G. A. Multiscale Simulations Reveal Key Features of the Proton-Pumping Mechanism in Cytochrome C Oxidase. *Proc. Natl. Acad. Sci. U. S. A.* **2016**, *113*, 7420−7425.
(119) Riistama, S.; Hummer, G.; Puustinen, A.; Dyer, R. B.; Woodruff, W. H.; Wikström, M. Bound Water in the Proton Translocation Mechanism of the Haem-Copper Oxidases. *FEBS Lett.* **1997**, *414*, 275−280.
(120) Maréchal, A.; Rich, P. R. Water Molecule Reorganization in Cytochrome C Oxidase Revealed by FTIR Spectroscopy. *Proc. Natl. Acad. Sci. U. S. A.* **2011**, *108*, 8634−8638.
(121) Ghosh, N.; Prat-Resina, X.; Gunner, M.; Cui, Q. Microscopic pK_a Analysis of Glu286 in Cytochrome C Oxidase (Rhodobacter sphaeroides): Toward a Calibrated Molecular Model. *Biochemistry* **2009**, *48*, 2468−2485.
(122) Woelke, A. L.; Galstyan, G.; Galstyan, A.; Meyer, T.; Heberle, J.; Knapp, E.-W. Exploring the Possible Role of Glu286 in C C O by Electrostatic Energy Computations Combined with Molecular Dynamics. *J. Phys. Chem. B* **2013**, *117*, 12432−12441.
(123) Wikström, M.; Verkhovsky, M. I. The D-Channel of Cytochrome Oxidase: An Alternative View. *Biochim. Biophys. Acta, Bioenerg.* **2011**, *1807*, 1273−1278.
(124) Maréchal, A.; Meunier, B.; Lee, D.; Orengo, C.; Rich, P. R. Yeast Cytochrome C Oxidase: A Model System to Study Mitochondrial Forms of the Haem−Copper Oxidase Superfamily. *Biochim. Biophys. Acta, Bioenerg.* **2012**, *1817*, 620−628.
(125) Iwata, S.; Ostermeier, C.; Ludwig, B.; Michel, H. Structure at 2.8 Angstrom Resolution of Cytochrome C Oxidase from Paracoccus Denitrificans. *Nature* **1995**, *376*, 660−669.
(126) Koepke, J.; Olkhova, E.; Angerer, H.; Müller, H.; Peng, G.; Michel, H. High Resolution Crystal Structure of Paracoccus Denitrificans Cytochrome C Oxidase: New Insights into the Active

DOI: 10.1021/acs.chemrev.7b00664
Chem. Rev. 2018, 118, 2469−2490

Site and the Proton Transfer Pathways. *Biochim. Biophys. Acta, Bioenerg.* **2009**, *1787*, 635−645.
(127) Soulimane, T.; Buse, G.; Bourenkov, G. P.; Bartunik, H. D.; Huber, R.; Than, M. E. Structure and Mechanism of the Aberrant Ba3-Cytochrome C Oxidase from Thermus Thermophilus. *EMBO J.* **2000**, *19*, 1766−1776.
(128) Tiefenbrunn, T.; Liu, W.; Chen, Y.; Katritch, V.; Stout, C. D.; Fee, J. A.; Cherezov, V. High Resolution Structure of the Ba3 Cytochrome C Oxidase from Thermus Thermophilus in a Lipidic Environment. *PLoS One* **2011**, *6*, e22348.
(129) Chang, H.-Y.; Hemp, J.; Chen, Y.; Fee, J. A.; Gennis, R. B. The Cytochrome Ba3 Oxygen Reductase from Thermus Thermophilus Uses a Single Input Channel for Proton Delivery to the Active Site and for Proton Pumping. *Proc. Natl. Acad. Sci. U. S. A.* **2009**, *106*, 16169−16173.
(130) Lee, H. J.; Gennis, R. B.; Ädelroth, P. Entrance of the Proton Pathway in Cbb3-Type Heme-Copper Oxidases. *Proc. Natl. Acad. Sci. U. S. A.* **2011**, *108*, 17661−17666.
(131) Sharma, V.; Wikström, M.; Kaila, V. R. Dynamic Water Networks in Cytochrome cbb3 Oxidase. *Biochim. Biophys. Acta, Bioenerg.* **2012**, *1817*, 726−734.
(132) Sharma, V.; Wikström, M. A Structural and Functional Perspective on the Evolution of the Heme−Copper Oxidases. *FEBS Lett.* **2014**, *588*, 3787−3792.
(133) Brochier-Armanet, C.; Talla, E.; Gribaldo, S. The Multiple Evolutionary Histories of Dioxygen Reductases: Implications for the Origin and Evolution of Aerobic Respiration. *Mol. Biol. Evol.* **2009**, *26*, 285−297.
(134) Richter, O. M.; Dürr, K. L.; Kannt, A.; Ludwig, B.; Scandurra, F. M.; Giuffre, A.; Sarti, P.; Hellwig, P. Probing the Access of Protons to the K Pathway in the Paracoccus Denitrificans Cytochrome C Oxidase. *FEBS J.* **2005**, *272*, 404−412.
(135) Woelke, A. L.; Galstyan, G.; Knapp, E.-W. Lysine 362 in Cytochrome C Oxidase Regulates Opening of the K-Channel Via Changes in Pk a and Conformation. *Biochim. Biophys. Acta, Bioenerg.* **2014**, *1837*, 1998−2003.
(136) Sharma, V.; Wikström, M. The Role of the K-Channel and the Active-Site Tyrosine in the Catalytic Mechanism of Cytochrome C Oxidase. *Biochim. Biophys. Acta, Bioenerg.* **2016**, *1857*, 1111−1115.
(137) Lyons, J. A.; Aragão, D.; Slattery, O.; Pisliakov, A. V.; Soulimane, T.; Caffrey, M. Structural Insights into Electron Transfer in Caa3-Type Cytochrome Oxidase. *Nature* **2012**, *487*, 514−518.
(138) Blomberg, M. R.; Siegbahn, P. E. Proton Pumping in Cytochrome C Oxidase: Energetic Requirements and the Role of Two Proton Channels. *Biochim. Biophys. Acta, Bioenerg.* **2014**, *1837*, 1165−1177.
(139) Carvalheda, C. A.; Pisliakov, A. V. Insights into Proton Translocation in cbb3 Oxidase from MD Simulations. *Biochim. Biophys. Acta, Bioenerg.* **2017**, *1858*, 396−406.
(140) Woelke, A. L.; Wagner, A.; Galstyan, G.; Meyer, T.; Knapp, E.-W. Proton Transfer in the K-Channel Analog of B-Type Cytochrome C Oxidase from Thermus Thermophilus. *Biophys. J.* **2014**, *107*, 2177−2184.
(141) Babcock, G. T.; Wikstrom, M. Oxygen Activation and the Conservation of Energy in Cell Respiration. *Nature* **1992**, *356*, 301.
(142) Ferguson-Miller, S.; Babcock, G. T. Heme/Copper Terminal Oxidases. *Chem. Rev.* **1996**, *96*, 2889−2908.
(143) Lindsay, J. G.; Wilson, D. F. Reaction of Cytochrome c Oxidase with CO: Involvement of the Invisible Copper. *FEBS Lett.* **1974**, *48*, 45−49.
(144) Chance, B.; Saronio, C.; Leigh, J. Functional Intermediates in the Reaction of Membrane-Bound Cytochrome Oxidase with Oxygen. *J. Biol. Chem.* **1975**, *250*, 9226−9237.
(145) Kitagawa, T.; Ogura, T. *Oxygen Activation Mechanism at the Binuclear Site of Heme−Copper Oxidase Superfamily as Revealed by Time-Resolved Resonance Raman Spectroscopy*; John Wiley & Sons, Inc.: Hoboken, NJ, 1996.
(146) Kaukonen, M. Calculated Reaction Cycle of Cytochrome C Oxidase. *J. Phys. Chem. B* **2007**, *111*, 12543−12550.
(147) Blomberg, M. R.; Siegbahn, P. E.; Babcock, G. T.; Wikström, M. Modeling Cytochrome Oxidase: A Quantum Chemical Study of the O− O Bond Cleavage Mechanism. *J. Am. Chem. Soc.* **2000**, *122*, 12848−12858.
(148) Schäfer, A.; Horn, H.; Ahlrichs, R. Fully Optimized Contracted Gaussian Basis Sets for Atoms Li to Kr. *J. Chem. Phys.* **1992**, *97*, 2571−2577.
(149) Schäfer, A.; Huber, C.; Ahlrichs, R. Fully Optimized Contracted Gaussian Basis Sets of Triple Zeta Valence Quality for Atoms Li to Kr. *J. Chem. Phys.* **1994**, *100*, 5829−5835.
(150) Sierka, M.; Hogekamp, A.; Ahlrichs, R. Fast Evaluation of the Coulomb Potential for Electron Densities Using Multipole Accelerated Resolution of Identity Approximation. *J. Chem. Phys.* **2003**, *118*, 9136−9148.
(151) Weigend, F.; Ahlrichs, R. Balanced Basis Sets of Split Valence, Triple Zeta Valence and Quadruple Zeta Valence Quality for H to Rn: Design and Assessment of Accuracy. *Phys. Chem. Chem. Phys.* **2005**, *7*, 3297−3305.
(152) Grimme, S.; Antony, J.; Ehrlich, S.; Krieg, H. A Consistent and Accurate Ab Initio Parametrization of Density Functional Dispersion Correction (Dft-D) for the 94 Elements H-Pu. *J. Chem. Phys.* **2010**, *132*, 154104.
(153) Becke, A. D. Density-Functional Exchange-Energy Approximation with Correct Asymptotic Behavior. *Phys. Rev. A: At., Mol., Opt. Phys.* **1988**, *38*, 3098.
(154) Perdew, J. P. Density-Functional Approximation for the Correlation Energy of the Inhomogeneous Electron Gas. *Phys. Rev. B: Condens. Matter Mater. Phys.* **1986**, *33*, 8822.
(155) Becke, A. D. Density-Functional Thermochemistry. Iii. The Role of Exact Exchange. *J. Chem. Phys.* **1993**, *98*, 5648−5652.
(156) Lee, C.; Yang, W.; Parr, R. G. Development of the Colle-Salvetti Correlation-Energy Formula into a Functional of the Electron Density. *Phys. Rev. B: Condens. Matter Mater. Phys.* **1988**, *37*, 785.
(157) Klamt, A.; Schüürmann, G. Cosmo: A New Approach to Dielectric Screening in Solvents with Explicit Expressions for the Screening Energy and Its Gradient. *J. Chem. Soc., Perkin Trans. 2* **1993**, *2*, 799−805.
(158) Ahlrichs, R.; Bär, M.; Häser, M.; Horn, H.; Kölmel, C. Electronic Structure Calculations on Workstation Computers: The Program System Turbomole. *Chem. Phys. Lett.* **1989**, *162*, 165−169.
(159) Verkhovsky, M. I.; Morgan, J. E.; Wikstroem, M. Oxygen Binding and Activation: Early Steps in the Reaction of Oxygen with Cytochrome C Oxidase. *Biochemistry* **1994**, *33*, 3079−3086.
(160) Verkhovsky, M. I.; Morgan, J. E.; Puustinen, A.; Wikstrom, M. Kinetic Trapping of Oxygen in Cell Respiration. *Nature* **1996**, *380*, 268−270.
(161) Blomberg, M. R. A.; Borowski, T.; Himo, F.; Liao, R.-Z.; Siegbahn, P. E. M. Quantum Chemical Studies of Mechanisms for Metalloenzymes. *Chem. Rev.* **2014**, *114*, 3601−3658.
(162) Wikström, M. Energy-Dependent Reversal of the Cytochrome Oxidase Reaction. *Proc. Natl. Acad. Sci. U. S. A.* **1981**, *78*, 4051−4054.
(163) Gorbikova, E. A.; Belevich, I.; Wikström, M.; Verkhovsky, M. I. The Proton Donor for Oo Bond Scission by Cytochrome C Oxidase. *Proc. Natl. Acad. Sci. U. S. A.* **2008**, *105*, 10733−10737.
(164) Blomberg, M. R.; Borowski, T.; Himo, F.; Liao, R.-Z.; Siegbahn, P. E. Quantum Chemical Studies of Mechanisms for Metalloenzymes. *Chem. Rev.* **2014**, *114*, 3601−3658.
(165) Rich, P. Towards an Understanding of the Chemistry of Oxygen Reduction. *Aust. J. Plant Physiol.* **1995**, *22*, 479−486.
(166) Jünemann, S.; Heathcote, P.; Rich, P. R. The Reactions of Hydrogen Peroxide with Bovine Cytochrome C Oxidase. *Biochim. Biophys. Acta, Bioenerg.* **2000**, *1456*, 56−66.
(167) Tommos, C.; Babcock, G. T. Proton and Hydrogen Currents in Photosynthetic Water Oxidation. *Biochim. Biophys. Acta, Bioenerg.* **2000**, *1458*, 199−219.
(168) Siletsky, S. A.; Belevich, I.; Jasaitis, A.; Konstantinov, A. A.; Wikström, M.; Soulimane, T.; Verkhovsky, M. I. Time-Resolved Single-Turnover of Ba 3 Oxidase from Thermus Thermophilus. *Biochim. Biophys. Acta, Bioenerg.* **2007**, *1767*, 1383−1392.

DOI: 10.1021/acs.chemrev.7b00664
Chem. Rev. 2018, 118, 2469−2490

(169) von Ballmoos, C.; Ädelroth, P.; Gennis, R. B.; Brzezinski, P. Proton Transfer in Ba 3 Cytochrome C Oxidase from Thermus Thermophilus. *Biochim. Biophys. Acta, Bioenerg.* **2012**, *1817*, 650−657.
(170) Andersson, R.; et al. Serial Femtosecond Crystallography Structure of Cytochrome C Oxidase at Room Temperature. *Sci. Rep.* **2017**, *7*, 4518.
(171) Hirata, K.; et al. Determination of Damage-Free Crystal Structure of an X-Ray-Sensitive Protein Using an Xfel. Nat. *Nat. Methods* **2014**, *11*, 734−736.
(172) Bloch, D.; Belevich, I.; Jasaitis, A.; Ribacka, C.; Puustinen, A.; Verkhovsky, M. I.; Wikström, M. The Catalytic Cycle of Cytochrome C Oxidase Is Not the Sum of Its Two Halves. *Proc. Natl. Acad. Sci. U. S. A.* **2004**, *101*, 529−533.
(173) Verkhovsky, M. I.; Jasaitis, A.; Verkhovskaya, M. L.; Morgan, J. E.; Wikström, M. Proton Translocation by Cytochrome C Oxidase. *Nature* **1999**, *400*, 480−483.
(174) Han, S.; Takahashi, S.; Rousseau, D. L. Time Dependence of the Catalytic Intermediates in Cytochromec Oxidase. *J. Biol. Chem.* **2000**, *275*, 1910−1919.
(175) Ishigami, I.; Hikita, M.; Egawa, T.; Yeh, S.-R.; Rousseau, D. L. Proton Translocation in Cytochrome C Oxidase: Insights from Proton Exchange Kinetics and Vibrational Spectroscopy. *Biochim. Biophys. Acta, Bioenerg.* **2015**, *1847*, 98−108.
(176) Wikström, M.; Verkhovsky, M. I. Towards the Mechanism of Proton Pumping by the Haem-Copper Oxidases. *Biochim. Biophys. Acta, Bioenerg.* **2006**, *1757*, 1047−1051.
(177) Gorbikova, E. A.; Vuorilehto, K.; Wikström, M.; Verkhovsky, M. I. Redox Titration of All Electron Carriers of Cytochrome C Oxidase by Fourier Transform Infrared Spectroscopy. *Biochemistry* **2006**, *45*, 5641−5649.
(178) Belevich, I.; Bloch, D. A.; Belevich, N.; Wikström, M.; Verkhovsky, M. I. Exploring the Proton Pump Mechanism of Cytochrome C Oxidase in Real Time. *Proc. Natl. Acad. Sci. U. S. A.* **2007**, *104*, 2685−2690.
(179) Kaila, V. R.; Johansson, M. P.; Sundholm, D.; Laakkonen, L.; Wikström, M. The Chemistry of the Cu B Site in Cytochrome C Oxidase and the Importance of Its Unique His−Tyr Bond. *Biochim. Biophys. Acta, Bioenerg.* **2009**, *1787*, 221−233.
(180) Blomberg, M. R. Mechanism of Oxygen Reduction in Cytochrome C Oxidase and the Role of the Active Site Tyrosine. *Biochemistry* **2016**, *55*, 489−500.
(181) Blomberg, M. R.; Siegbahn, P. E. Protonation of the Binuclear Active Site in Cytochrome C Oxidase Decreases the Reduction Potential of Cub. *Biochim. Biophys. Acta, Bioenerg.* **2015**, *1847*, 1173−1180.
(182) Wikström, M. Identification of the Electron Transfers in Cytochrome Oxidase That Are Coupled to Proton-Pumping. *Nature* **1989**, *338*, 776−778.
(183) Wikström, M.; Krab, K. Proton-Pumping Cytochrome c Oxidase. *Biochim. Biophys. Acta, Rev. Bioenerg.* **1979**, *549*, 177−222.
(184) Morgan, J. E.; Verkhovsky, M. I.; Wikström, M. The Histidine Cycle: A New Model for Proton Translocation in the Respiratory Heme-Copper Oxidases. *J. Bioenerg. Biomembr.* **1994**, *26*, 599−608.
(185) Siletsky, S. A.; Konstantinov, A. A. Cytochrome C Oxidase: Charge Translocation Coupled to Single-Electron Partial Steps of the Catalytic Cycle. *Biochim. Biophys. Acta, Bioenerg.* **2012**, *1817*, 476−488.
(186) Popović, D. M.; Stuchebrukhov, A. A. Proton Pumping Mechanism and Catalytic Cycle of Cytochrome C Oxidase: Coulomb Pump Model with Kinetic Gating. *FEBS Lett.* **2004**, *566*, 126−130.
(187) Siletsky, S. A.; Pawate, A. S.; Weiss, K.; Gennis, R. B.; Konstantinov, A. A. Transmembrane Charge Separation During the Ferryl-Oxo→ Oxidized Transition in a Nonpumping Mutant of Cytochrome C Oxidase. *J. Biol. Chem.* **2004**, *279*, 52558−52565.
(188) Wikström, M.; Bogachev, A.; Finel, M.; Morgan, J. E.; Puustinen, A.; Raitio, M.; Verkhovskaya, M.; Verkhovsky, M. I. Mechanism of Proton Translocation by the Respiratory Oxidases. The Histidine Cycle. *Biochim. Biophys. Acta, Bioenerg.* **1994**, *1187*, 106−111.
(189) Quenneville, J.; Popović, D. M.; Stuchebrukhov, A. A. Redox-Dependent P K a of Cub Histidine Ligand in Cytochrome C Oxidase. *J. Phys. Chem. B* **2004**, *108*, 18383−18389.
(190) Wikström, M.; Verkhovsky, M. I. Mechanism and Energetics of Proton Translocation by the Respiratory Heme-Copper Oxidases. *Biochim. Biophys. Acta, Bioenerg.* **2007**, *1767*, 1200−1214.
(191) Kaila, V. R.; Sharma, V.; Wikström, M. The Identity of the Transient Proton Loading Site of the Proton-Pumping Mechanism of Cytochrome C Oxidase. *Biochim. Biophys. Acta, Bioenerg.* **2011**, *1807*, 80−84.
(192) Siegbahn, P. E.; Blomberg, M. R.; Blomberg, M. L. Theoretical Study of the Energetics of Proton Pumping and Oxygen Reduction in Cytochrome Oxidase. *J. Phys. Chem. B* **2003**, *107*, 10946−10955.
(193) Supekar, S.; Gamiz-Hernandez, A. P.; Kaila, V. R. I. A Protonated Water Cluster as a Transient Proton-Loading Site in Cytochrome C Oxidase. *Angew. Chem., Int. Ed.* **2016**, *55*, 11940−11944.
(194) Lu, J.; Gunner, M. R. Characterizing the Proton Loading Site in Cytochrome C Oxidase. *Proc. Natl. Acad. Sci. U. S. A.* **2014**, *111*, 12414−12419.
(195) Ädelroth, P.; Gennis, R. B.; Brzezinski, P. Role of the Pathway through K (I-362) in Proton Transfer in Cytochrome C Oxidase from R. *Biochemistry* **1998**, *37*, 2470−2476.
(196) Lepp, H.; Salomonsson, L.; Zhu, J.-P.; Gennis, R. B.; Brzezinski, P. Impaired Proton Pumping in Cytochrome C Oxidase Upon Structural Alteration of the D Pathway. *Biochim. Biophys. Acta, Bioenerg.* **2008**, *1777*, 897−903.
(197) Faxén, K.; Gilderson, G.; Ädelroth, P.; Brzezinski, P. A Mechanistic Principle for Proton Pumping by Cytochrome C Oxidase. *Nature* **2005**, *437*, 286.
(198) Siegbahn, P. E.; Blomberg, M. R. Energy Diagrams and Mechanism for Proton Pumping in Cytochrome C Oxidase. *Biochim. Biophys. Acta, Bioenerg.* **2007**, *1767*, 1143−1156.
(199) Brzezinski, P.; Larsson, G. Redox-Driven Proton Pumping by Heme-Copper Oxidases. *Biochim. Biophys. Acta, Bioenerg.* **2003**, *1605*, 1−13.
(200) Yang, S.; Cui, Q. Glu-286 Rotation and Water Wire Reorientation Are Unlikely the Gating Elements for Proton Pumping in Cytochrome C Oxidase. *Biophys. J.* **2011**, *101*, 61−69.
(201) Kaila, V. R.; Verkhovsky, M. I.; Hummer, G.; Wikström, M. Glutamic Acid 242 Is a Valve in the Proton Pump of Cytochrome C Oxidase. *Proc. Natl. Acad. Sci. U. S. A.* **2008**, *105*, 6255−6259.
(202) Pawate, A. S.; Morgan, J.; Namslauer, A.; Mills, D.; Brzezinski, P.; Ferguson-Miller, S.; Gennis, R. B. A Mutation in Subunit I of Cytochrome Oxidase from Rhodobacter Sphaeroides Results in an Increase in Steady-State Activity but Completely Eliminates Proton Pumping. *Biochemistry* **2002**, *41*, 13417−13423.
(203) Vakkasoglu, A. S.; Morgan, J. E.; Han, D.; Pawate, A. S.; Gennis, R. B. Mutations Which Decouple the Proton Pump of the Cytochrome C Oxidase from Rhodobacter Sphaeroides Perturb the Environment of Glutamate 286. *FEBS Lett.* **2006**, *580*, 4613−4617.
(204) Johansson, A.-L.; Carlsson, J.; Högbom, M.; Hosler, J. P.; Gennis, R. B.; Brzezinski, P. Proton Uptake and P K a Changes in the Uncoupled Asn139cys Variant of Cytochrome C Oxidase. *Biochemistry* **2013**, *52*, 827−836.
(205) Han, D.; Namslauer, A.; Pawate, A.; Morgan, J. E.; Nagy, S.; Vakkasoglu, A. S.; Brzezinski, P.; Gennis, R. B. Replacing Asn207 by Aspartate at the Neck of the D Channel in the Aa3-Type Cytochrome C Oxidase from Rhodobacter Sphaeroides Results in Decoupling the Proton Pump. *Biochemistry* **2006**, *45*, 14064.
(206) Yoshikawa, S.; Muramoto, K.; Shinzawa-Itoh, K. Proton-Pumping Mechanism of Cytochrome C Oxidase. *Annu. Rev. Biophys.* **2011**, *40*, 205−223.
(207) Shimada, A. A Nanosecond Time-Resolved Xfel Analysis of Structural Changes Associated with Co Release from Cytochrome C Oxidase. *Sci. Adv.* **2017**, *3*, e1603042.
(208) Papa, S.; Capitanio, G.; Papa, F. The Mechanism of Coupling between Oxido-Reduction and Proton Translocation in Respiratory Chain Enzymes. *Biol. Rev.* **2017**, 12347.

DOI: 10.1021/acs.chemrev.7b00664
Chem. Rev. 2018, 118, 2469−2490

(209) Egawa, T.; Yeh, S.-R.; Rousseau, D. L. Redox-Controlled Proton Gating in Bovine Cytochrome C Oxidase. *PLoS One* **2013**, *8*, e63669.
(210) Salje, J.; Ludwig, B.; Richter, O. M. H. Is a Third Proton-Conducting Pathway Operative in Bacterial Cytochrome c Oxidase? *Biochem. Soc. Trans.* **2005**, *33*, 829.
(211) Rich, P. R. *Cytochrome c Oxidase: Insight into Functions from Studies of the Yeast S. Cerevisiae Homologue*; World Scientific Publishers: London, UK, 2017.
(212) Yoshikawa, S.; Muramoto, K.; Shinzawa-Itoh, K.; Mochizuki, M. Structural Studies on Bovine Heart Cytochrome C Oxidase. *Biochim. Biophys. Acta, Bioenerg.* **2012**, *1817*, 579−589.
(213) Yano, N.; et al. The Mg2+-Containing Water Cluster of Mammalian Cytochrome C Oxidase Collects Four Pumping Proton Equivalents in Each Catalytic Cycle. *J. Biol. Chem.* **2016**, *291*, 23882−23894.
(214) Muramoto, K.; Ohta, K.; Shinzawa-Itoh, K.; Kanda, K.; Taniguchi, M.; Nabekura, H.; Yamashita, E.; Tsukihara, T.; Yoshikawa, S. Bovine Cytochrome C Oxidase Structures Enable O2 Reduction with Minimization of Reactive Oxygens and Provide a Proton-Pumping Gate. *Proc. Natl. Acad. Sci. U. S. A.* **2010**, *107*, 7740−7745.
(215) Sharma, V.; Jambrina, P. G.; Kaukonen, M.; Rosta, E.; Rich, P. R. Insights into Functions of the H Channel of Cytochrome C Oxidase from Atomistic Molecular Dynamics Simulations. *Proc. Natl. Acad. Sci. U. S. A.* **2017**, *114*, E10339−E10348.
(216) Artzatbanov, V. Y.; Konstantinov, A.; Skulachev, V. Involvement of Intramitochondrial Protons in Redox Reactions of Cytochrome A. *FEBS Lett.* **1978**, *87*, 180−185.
(217) Capitanio, N.; Capitanio, G.; Boffoli, D.; Papa, S. The Proton/Electron Coupling Ratio at Heme a and Cua in Bovine Heart Cytochrome C Oxidase. *Biochemistry* **2000**, *39*, 15454−15461.
(218) Capitanio, N.; Capitanio, G.; Minuto, M.; De Nitto, E.; Palese, L. L.; Nicholls, P.; Papa, S. Coupling of Electron Transfer with Proton Transfer at Heme a and Cua (Redox Bohr Effects) in Cytochrome C Oxidase. Studies with the Carbon Monoxide Inhibited Enzyme. *Biochemistry* **2000**, *39*, 6373−6379.
(219) Capitanio, N.; Vygodina, T. V.; Capitanio, G.; Konstantinov, A. A.; Nicholls, P.; Papa, S. Redox-Linked Protolytic Reactions in Soluble Cytochrome-C Oxidase from Beef-Heart Mitochondria: Redox Bohr Effects. *Biochim. Biophys. Acta, Bioenerg.* **1997**, *1318*, 255−265.
(220) Verkhovsky, M. I.; Belevich, N.; Morgan, J. E.; Wikström, M. Proton Linkage of Cytochrome a Oxidoreduction in Carbon Monoxide-Treated Cytochrome C Oxidase. *Biochim. Biophys. Acta, Bioenerg.* **1999**, *1412*, 184−189.
(221) Ellis, W. R., Jr; Wang, H.; Blair, D. F.; Gray, H. B.; Chan, S. I. Spectroelectrochemical Study of the Cytochrome a Site in Carbon Monoxide Inhibited Cytochrome C Oxidase. *Biochemistry* **1986**, *25*, 161−167.
(222) Ingledew, W. J. Structure and Function of Energy-Transducing Membranes: Edited by K. Van Dam and B. F. Van Gelder. (Bba Library, Vol. 14) Pp. 342. Elsevier Scientific Publishing Company, Amsterdam and New York. 1978, $41.95 or Dfl. 103 00. *Biochem. Educ.* **1978**, *6*, 90−90.
(223) Krab, K.; Slater, E. Ferrocyanide as Electron Donor to Cytochrome aa_3. Cytochrome C Requirement for Oxygen Uptake. *Biochim. Biophys. Acta, Bioenerg.* **1979**, *547*, 58−69.

DOI: 10.1021/acs.chemrev.7b00664
Chem. Rev. 2018, 118, 2469−2490